IAARHIES
Governed by:The Society for Academic Research
www.iaarhies.org

Journal of Innovative Research in Clinical & Medical Sciences

International Peer reviewed Scientific Journal

Vol. 1 ISSN 2456-7736 Issue: II

Issued by: The Society for Academic Research (Regd.)

www.ijircms.com

IAARHIES International Journal of Innovative Research in Clinical & Medical Sciences

International peer-reviewed Scientific Journal

Volume - 1 Special Edition - II Oct., 2017 ISSN – 2456-7736

Published by:

IAARHIES

Governed by The Society for Academic Research®

www.iaarhies.org

The Society for Academic Research (Regd.)

Impact Factor (SJIF)

4.682 (2017)

Office Address:

The Society for Academic Research (Regd.)

Address: A-65, Gol Market, Jawahar Nagar, Jaipur-302004, Raj (India)

Helpline: +91-7231050000, +91(0)141 2654500

Email: **info@iaarhies.org** Web: **www.iaarhies.org**

Website: www.iaarhies.org

Publisher: The Society for Academic Research (Regd),
Jawahar Nagar, Jaipur, 302004 (Rajasthan)

Disclaimer
Views expressed in this journal are those of the contributors and are not of the publishers/editors.

ISSN – 2456-7736

Type set:
IT Team - (IAARHIES) & Computer World, New Delhi, India

Editorial Board

CONTENTS

Photocatalytic Degradation of Janus Green B Using Cobalt Hexacyanoferrate (II) as Semiconductor

R.K. Sharma*, Seema Yadav, R.K. Vijai**, Reema Upadhyay[†],**
*Department of Physics, M.S.J. Govt. College, Bharatpur (Rajasthan),
**Department of Physics, R.R. Govt. College, Alwar (Rajasthan),
[†]Department of Chemistry, J.K. College of Science and Research Technology, Bharatpur (Raj.)

Abstract: The Photocatalytic degradation of Janus green-B has been investigated using Cobalt hexacyanoferrate (II) as semiconductor. Cobalt hexacyanoferrate (II) was used as effective photo catalysts for carrying out number of chemical reactions. The photo catalytic bleaching of Janus green-B was carried out in the presence of semi conducting Cobalt hexacyanoferrate and the progress of the reaction was observed spectrophotometrically. The effects of various operating variables like pH, concentration of dyes, amount of semiconductor and light intensity on the rate of bleaching was observed. A tentative mechanism has been proposed for the photo catalytic bleaching of dyes.

Key words: - Photocatalytic degradation, Cobalt hexacyanoferrate (II), Janus green – B.

INTRODUCTION

A number of studies have been concentrated on the degradation of toxic dyes in waste water via photocatalysis using various semiconductors like oxides, sulphides, and complexes of transition metal ions. Nanoparticles of TiO_2 were used by Chen et al.[1] in UV light induced photodegradation of malachite green. Degradation of Janus green B dye in aqueous medium using Ammonium phosphomolybdate has been assisted by Sharma et al.[2], Mills et *al*.[3] used CdS and Vaya et al.[4] used ZnS in photocatalytic degradation of Methyl orange and Eosin-Y respectively. Other oxide, e.g. TiO_2/ZnO[5], MnO_2[6,7] and sulphides, e.g. NiS-ZnS[8] are also used as photocatalyst.

Presently, different transition metal complexes play an important role in photocatalytic degradation of different dyes. Talk et al.[9] used Copper hexacyanoferrate (II) as photocatalyst for photocatalytic bleaching of Rose Bengal and Bismark brown. Sharma et al.[10] studies the photocatalytic degradation of Amidoblack-10B using copper hexacyanoferrate (II). Ali et al.[11] showed the catalytic activity of Nickel hexacyanoferrate (II) in the degradation of Benzyl alcohol. Sharma et al.[12,13] also used Nickel hexacyanoferrate (II) and Cobalt hexacynoferrate (II) for photodegradation of AmidoBlack-10 and neutral red dye respectively.

From the literature survey, it is apparent that very little attention has paid on Cobalt hexacyanoferrate (II) as semiconductor for photocatalytic degradation, which is coloured, insoluble in water and able to utilize sun light efficiently.

In the present study cobalt hexacyanoferrate (II) is used as semiconductor in the photocatalytic degradation of Janus green B dye. Janus green B is a basic dye and vital stain used in histology. It is also used to mitochondria supravitally. The Chemical Structure of Janus green B is-

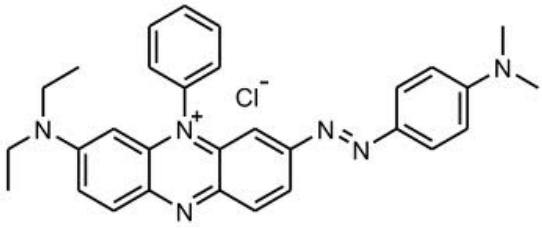

EXPERIMENTAL

Material and methods

The stock solution (1.0×10^{-3}M) of Janus green B was prepared in double distilled water (500mL) and further diluted as and when required. The pH of the solution was maintained by addition previously

standarised H_2SO_4 and NaOH solution and measured by digital pH meter (Systronics, Model 335). 0.06g of cobalt hexacyanoferrate (II) was added to 50.0mL for 2.4×10^{-5}M Janus green B solution. The solution was exposed by a 200 W tungsten lamp (Philips).The intensity of light was measured by a solar meter (Surya mapi CEL model 201). A water filter was used to remove thermal degradation. The optical density of solution was recorded at regular time interval by using Spectrophotometer (Systronics-104). Before measuring OD, cobalt hexacyanoferrate (II) was removed by the help of centrifuging Machine (Remi, Model 1258).

RESULTS AND DISCUSSION

Photocatalytic degradation of Janus green B was observed at $\lambda_{max} = 620$ nm. A graph, plotted between exposure time and 1 + log OD is obtained as straight line, which indicates that photocatalytic degradation of Janus green B follow pseudo first order kinetics. The rate constant k for the reaction was determined using the expression.

$$\mathbf{k = 2.303 \times slope}$$

The results for a typical run are presented in Table 1 and graphically represented in Fig.1.

Table1: A Typical run

[Janus green B] = 2.4×10^{-5} M pH = 11.5
Cobalt hexacyanoferrate (II) = 0.06g Light intensity = 51.0mWcm^{-2}

Time (min.)	Optical density	1 + log O.D.
0	0·851	0·929
20	0·618	0·791
40	0·457	0·660
60	0·342	0·535
80	0·258	0·412
100	0·191	0·281
120	0·145	0·161
		k = 2.45×10^{-4} sec^{-1}

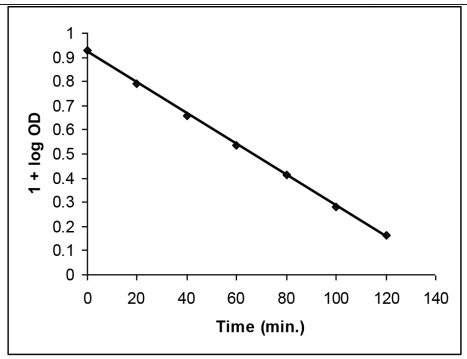

Fig. 1: A typical run

Effect of pH

The pH of solution is likely to affect the photocatalytic bleaching of the dye and hence, the effect of pH on the rate of dye solution was investigated in the pH range (9.5 to13). The results are recorded in the table 2 and graphically presented in fig. 2.

Table 2: Effect of pH

[Janus green B] = 2.4×0^{-5} M Cobalt hexacyanoferrate (II) = 0.06g
Light intensity = 51.0mWcm^{-2}

pH	k ×10⁴ (sec⁻¹)
9·5	1.94
10·0	2·04
10·5	2.15
11·0	2.35
11·5	2.45
12·0	2.41
12·5	2.38
13·0	2.35

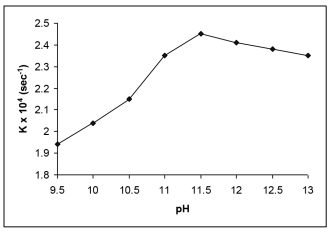

Fig. 2: Effect of pH

It is evident from the above data that the rate of the photocatalytic bleaching of Janus green B increases with increase in pH up to pH = 11.5. It is due to more availability of the OH^- ion at higher pH values. These OH^- ions combine with the hole to form $^{\bullet}OH$ radicals, thus more OH^- will generate more $^{\bullet}OH$ radicals. These hydroxyl free radicals are responsible for this photocatalytic degradation. On increasing the pH above pH =11.5, rate of degradation of dye decreases, as the pH of the solution is increased, more OH^- ion will be available and these ions are absorbed on the surface of semiconductor making it negatively charged and as a consequence of repulsive force between two negatively charged species (OH^- ion and electron rich dye), the approach of electron rich dye to the semiconductor surface will be retarded. This will result into decrease in the rate of photocatalytic degradation of Janus green B.

Effect of Janus green B concentration

The effect of variation of Janus green B concentration on the rate of reaction was observed by using different concentration of Janus green B. The results are reported in table 3 and graphically presented in fig.3.

Table 3: Effect of Janus green B concentration

Cobalt hexacyanoferrate (II) = 0.06gm
Light intensity = 51.0m Wcm^{-2} pH = 11.5

[Janus green B] × 10^5M	k ×10^4(Sec^{-1})
1.2	1.80
1·6	1.92
2.0	2.11
2·4	2.45
2·8	2.21
3.2	2·15
3·6	2·01

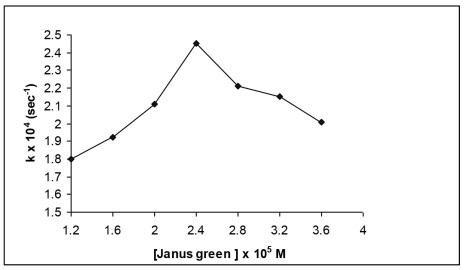

Fig.3: Effect of dye concentration

It has been observed that the rate of photocatalytic degradation increases with an increase in the concentration of dye up to 2.4×10^{-5} M. Further increase in concentration of dye resulted into decrease in the rate of photocatalytic degradation. It may be explained on the basis of the fact as the concentration of dye was increased, more dye molecules will be available excitation and for consecutive energy transfer, hence increase in the rate of photocatalytic degradation is observed. But when the concentration of Janus green B is increased above 2.4×10^{-5} M, the dye itself will start acting as a filter for incident light. It does not permit the desired light intensity to rich the semiconductor surface; Thus decreasing the rate of photocatalytic degradation of Janus green B.

Effect of amount of semiconductor

The effect of amount of Cobalt hexacyanoferrate (II) powder on the rate of photocatalytic degradation of Janus green B was observed and therefore, the amount of SC was varied from 0.02g to 0.14g keeping all the factor were identical. The results are reported in table 4 and graphically presented in fig. 4.

Table 4: Effect of amount of semiconductor

[Janus green B] = 2.4×10^{-5} M

Light intensity= 51.0 m W cm^{-2} pH = 11.5

Amount of Cobalt hexacyanoferrate (II) (g.)	$k \times 10^4$ (Sec^{-1})
0·02	1·81
0·04	2·11
0·06	2.45
0·08	2.45
0·10	2.45
0·12	2.44
0·14	2.43

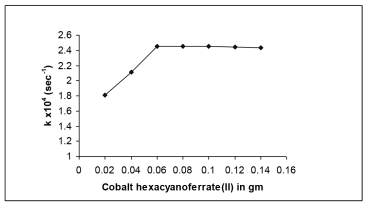

Fig.4: Effect of amount of semiconductor

As indicated from above data, it is observed that rate of photocatalytic degradation of dye increases with increase in the amount of cobalt hexacyanoferrate (II) up to 0.06 gm. but beyond 0.06 g, the rate of reaction becomes virtually constant. This can be explained on the fact that, as the amount of semiconductor is increased exposed surface area of SC will also increased, thus an increase in the rate of reaction is observed. But, after certain limiting amount of SC (0.06g), if the amount of SC was further increased, it will not contribute to an increase in the exposed surface area. On the contrary, it will increase only the thickness of SC powder at the bottom of reaction. This will also confirmed by using reaction vessels of different dimensions. Thus, after certain amount of SC, the saturation point reached.

Effect of intensity of light

To observe the effect of light intensity, all other factors were kept constant. The effect of variation of light intensity on the rate of photocatalytic degradation of Janus green B was also observed. The results are reported in table 5 and graphically presented figure 5.

Table 5: Effect of light intensity

[Janus green B] = 2.4×10^{-5} M Cobalt hexacyanoferrate (II) = 0.06g
pH =11.5

Light intensity in $mWcm^{-2}$	$k \times 10^4$(sec^{-1})
35	1.58
38	1.71
41	1.81
44	1.92
47	2.11
50	2·29
51	2.45

As indicated from the data, it is observed that rate of photocatalytic degradation of Janus green B increases on the increasing the intensity of light from 35 $mWcm^{-2}$ to 51 $mWcm^{-2}$. It may be explained on the basis of that as the light intensity is increased, the number of photon striking per unit area of SC are also increased. Thus increase in the rate of photocatalytic reaction is observed and a linear behaviour between light intensity and rate of reaction is observed. However, higher intensities are avoided due to thermal effect

Mechanism

On the basis of experimental observation a tentative mechanism has been proposed for degradation of Janus green B by Cobalt hexacyanoferrate (II).

$$^{1}Dye_{0} + h\nu \longrightarrow {}^{1}Dye_{1} \text{ (Singlet excited state)} \quad \ldots(1)$$

$$^{1}Dye_{1} \xrightarrow{ISC} {}^{3}Dye_{1} \text{ (triplet excited state)} \quad \ldots(2)$$

$$SC + h\nu \longrightarrow e^{-} + h^{+} \text{ or } SC^{*} \quad \ldots(3)$$

$$h^{+} + OH^{-} \text{ (from base)} \longrightarrow {}^{\bullet}OH \quad \ldots(4)$$

$$^{3}Dye_{1} + {}^{\bullet}OH \longrightarrow \text{Product} \quad \ldots(5)$$

When solution of dye was exposed to light in presence of semiconductor; initially, the dye molecules were excited first to their excited singlet state. These excited state molecules were converted to the triplet state through inter system crossing (I SC). Semiconductor also utilize radiant energy to excite its electron from valence band to conduction band; thus living behind a hole. This hole abstracts an electron from OH^{-} ions generating $^{\bullet}OH$ free radical. The dye is bleached by this $^{\bullet}OH$ radical.

CONCLUSION

Janus green B dye can be successfully degraded using cobalt hexacyanoferrate (II) semiconductor under visible light irradiation. Thus cobalt hexacyanoferrate (II) may act as a photocatalyst quite effectively to photodegrade different dye molecules to colourless less toxic products.

REFERENCES

1. Chen, C.C., Lu, C.S., Chung, Y.C. and Jan, J.L., UV light Induced photodegradation of malachite green on TiO2 nanoparticles, *J. Hazardous Material,* 141, 520, 2007.
2. Sharma, S., Chaturvedi, N., Sharma, M.K.and Chaturvedi, R.K, Decolorization of Janus green in aqous solution employing Ammonium phosphomolybdate semiconductor, *Jr. of Industrial Pollution Control, 193, 2010.*
3. Mills, A. and Williams, G., Methyl orange as a probe of the semiconductor-electrolyte interface in CdS suspensions, *J. Chem. Faraday Trans.* 183(8), 2647, 1987.
4. Vaya, D., Vyas, R., Ameta, R. and Sharma, V.K., Use of modified ZnS in Photocatlytic bleaching of Eosin-Y, J. *Indian Chem. Soc.*85,1266,2008.
5. Liao, D.C., Badour, C.A. and Liao, B.Q., Preparation of nanosized TiO_2/ZnO composite catalysis and its photocatalytic activity for degradation of methyl orange, *J. Photochem. Photobiol,* 194a, 11, 2008.
6. Sharma, S., Chaturvedi, N., Sharma, M.K.and Chaturvedi, R.K., Decolorization of Safranine O in aqous solution employing manganese dioxide semiconductor EM, *Jr. of Industrial Pollution Control,* 30 (2), 165, 2011.
7. Ameta, K.L., Malkani, R.K. and Ameta, S.C., Use of semiconducting a Maganecium (IV) oxide particulate system as a photocatalyst: photoassisted bleaching of some dyes, *Int. J. Chem. Sci., 8(3),*1658, 2010.
8. Sharma, V., Gandhi, N., Khant, A. and Khandelwal, R.C., Role of coprecipitated NiS-ZnS in Photocatalytic degradation of Alzarin red, *Int. J. Chem. Sci,* 8(2), 961, 2010.
9. Tak, P., Ameta, A., Ameta, R., Sharma, V.K. and Panjabi, P.B., Use of photocatalytic degradation of Bismark brown, Int. *J. Chem. Sci.*8(1), 351,2010

10. Sharma, O.P., Sharma, M., Sharma, M.K. and Upadhyay, D.U., Photochemical degradation of Amidoblack-10B using copper hexacyanoferrate (II) as semiconductor, *Int. J. of Chem. Sci,* 10 (2), 956, 2012.
11. Ali, S.R., Chandra, P., Latwal, M., Jain, S.K., Bansal, V.K. and Singh, Synthesis of Nickel hexacyanoferrate nanoparticles and their potential as a heterogeneous catalysis for the solventfree oxidationof benzyl alcohol, *chin. Jr. Catal,* 32 (12), 2011.
12. Sharma, O.P., Sharma, M., Sharma, M.K. and Upadhyay, D.U., Photochemical degradation of Amidoblack-10B using nickel hexacyanoferrate (II) as semiconductor, *Jr. of Industrial Pollution Control*, 28 (2), 171, 2012.
13. Sharma, O.P. and Sharma, M.K., Use of Cobalt hecacynoferrate (II) semiconductor in photocatalytic degradation of neutral red dye, International Journal of Chem Tech Research, 5 (4), 1615-22, 2013.

Avian Diversity of Silised Wetland Alwar, Rajasthan

Niraj and Ajay Kumar

Wild Life Research Lab, Deptt. of Zoology,

Raj Rishi Govt. P. G. College, Alwar (Rajasthan)

E mail-drajayzoology@gmail.com

INTRODUCTION:

wetlands are the transitional zones between permanently aquatic and dry terrestrial ecosystems. They have profound ecological and economic importance. Mostly they are highly productive but ecologically fragile, liable to degradation and degeneration under the prevailing anthropogenic pressure which in turn affects the avian diversity around them.

Apart from their beauty, recreational and economic importance, wetland birds are excellent indicators of the general health of an ecosystem and measure of its biodiversity. India has 243 species of water-birds and 67 species of wetland dependent and associated birds (Kumar et al. 2005), almost half of these are migratory and visit India from their breeding grounds in China, Russia, central Asia, Tibet and from across the entire range of the Himalaya. The availability of feeding and roosting habitats is very important for these migratory species, which in some cases migrate up to thousands of kilometers. As wetlands provide a wintering ground for many trans-equatorial species of migratory birds, several wetlands in the country have been identified as being internationally significant under the Ramsar Convention.

In Rajasthan winter season is the most flourishing season and it invites numerous migratory birds from far off places. Some of the migratory birds flocking in to this region are common crane, ducks, coots, pelicans and the Siberian cranes, imperial sand grouse, falcons and buzzards.

The present studies assess the avian diversity of Silised wetland, 63 species of birds observed, belonging to 10 orders and 15 families. All these birds depend upon wetland flora and fauna along with the nearby crop fields for their food. Anthropogenic activities have resulted in over exploitation of wetland resources, thus affecting the advent of avifauna.

Present study is not carried out only to prepare the check list of birds but to find out their occurrence and to create the awareness for their conservation.

STUDY AREA:

Silised Lake is situated about 13 kms south-west of Alwar city in Rajasthan (India). It was constructed by Maharaja Vinay Singh in the year 1845 on a tributary of Ruparel. Its storage capacity is 492 million cubic feet and the catchment area is about 1124 Ha. It also irrigates some agricultural land every year. The topography of study area supports scrub-thorny arid forests, dry deciduous forests, rocks and grasses. The study area being a part of the Aravalli Range, is rich in mineral resources.

METHODS AND DATA ANALYSIS:

Bird watching and recording has been carried out for a period of two years (2010- 2012). A field binoculars and GPS were used throughout the study period for observation of the Avifauna in the study area. Photography was done with Sony camera with Zoom lenses. The avifauna of Silised Lake was studied through systematic large–scale surveys utilizing point counts as well as opportunistic observations throughout the study period. Recorded birds were identified by using standard books such as Ali, S. & Ripley (1987) and Grimmett, et al (1999).

Birds inhabiting wetlands for feeding, breeding, nesting or roosting are broadly defined as water birds. This comprises bird groups commonly called waterfowl and waders. In addition, several other bird groups like kingfishers, raptors and some passerines are also ecologically dependent on wetlands, hence known as wetland dependent and associated birds (Kumar et al. 2005). In this paper, water birds, wetland

dependent and associated birds are collectively termed as wetland birds. Monitoring of wetland birds provides valuable information on the ecological health and status of wetlands and can be a vital tool for developing awareness regarding the conservation value of the wetlands.

The term 'waterfowl' applies to the members of the family Anatidae, popularly known as Swans, Geese and Ducks, the smallest of which are called Teals. A total of 149 species are known to occur throughout the world, of which 41 from India (Ali & Ripley, 1978). It is known that every waterfowl is a water bird, but every water bird is not a waterfowl. In the recent past, the term waterfowl has been frequently used in a broader perspective covering water birds as well, (Tak et al, 2003).

OBSERVATION AND RESULT:

In this study total 63 species of wetland birds, belonging to10 orders and 15 families have been recorded at Silised wetland (Table-1). This wetland also has 48 species of water dependant birds, belonging to 13 families.

The waterbirds generally include swimmers, divers and waders. The two belong to the following four families, viz, Podicipedidae, Phalacrocoracidae, Anatidae, Larvidae. While the waders (marsh birds) belong to the following families, viz, Ardeidae, Charadriidae, Recurvirostridae, Gruidae, Rallidae, Ciconiidae, Jacanidae, Threskiornithidae and Burhinidae.

Waders (Marsh birds) like Pond herons, Purple herons, Avocets, Greenshank, Red wettled lapwing, Black winged stilt, Little ringed plover, Shanks, Curlews, Sand pipers and Cattle egrets were seen to prefer shallow muddy banks of the pond and close by small water spots

The wetland dependent birds such as Kites, Eagles, Vultures and Kingfishers were also seen around the Silised wetland. They built their nest usually on lofty trees preferably near water. During winter months they prey on variety of water birds.

The trees species of Prosopis cineria, Prosopis Juliflora, Azardir indica, Tecomella undulata (rachta), Nerium oleander, Calotropis procera present at the banks of the wetlands give shelter to common terrestrial residential birds like Parrots, Babblers, Mynas, Doves, Bulbuls, Patridges and Drongos. These birds were also found feeding on the grains scattered by local population.

At Silised wetland intense human activities has been seen. This Lake is being used for swimming, for irrigation, boating and fishing. These activities disturb the water birds in the Lake. Direct observations as well as personal interviews with local people during surveys revealed that anthropogenic activities like livestock grazing, soil digging, encroachment, use of forest wood as a source of fuel by local people, cutting of emergent and fringed vegetation are some of the major threats to the biodiversity of this wetland.

CONCLUSION:

It is concluded that silised wetland have great avian diversity including resident and migratory species. But the avian heritage of this wetland is under threat due to increased anthropogenic activities resulting in habitat destruction and fragmentation. It is an alarming sign for conservation of the avian diversity of this wetland. Regular surveys related to waterbird species diversity and awareness of the local people should be conducted for a detailed assessment of the wetland.

Table-1

Sr. no.	Common name	Scientific name	Resident---ial status	Abund---ance status	Conser--vation status IUCN/ CITES 2002	WL(P) A 1972
	Grebe	**Order- Podicipediformes**	**Family-Podicipedidae**			
1	Little Grebe	Tachybaptus ruficollis	R/LM	Com		Sch. IV
	Pelican	**Order- Pelecaniformes**	**Family- Pelecanidae**			
2	Great White Pelican	Pelecanus onocrotalus	R/WM	LCom		Sch. IV

3	Spot-billed Pelican	Pelecanus philippensis	R/LM	LCom	GT/Vu	Sch. IV
	Cormorants/Shags	**Order- Pelecaniformes**	**Family- Phalacrocoracidae**			
4	Little Cormorant	Phalacrocorax niger	R/LM	Com		Sch. IV
5	Indian Shag	Phalacrocorax fuscicollis	R/LM	Com		Sch. IV
6	Great Cormorant	Phalacrocorax carbo	R/WM	Com		Sch. IV
	Darter	**Order- Pelecaniformes**	**Family- Anhingidae**			
7	Darter	Anhinga melanogaster	R/LM	LCom	NT	Sch. IV
	Herons, Egrets	**Order-Ciconiformes**	**Family -Ardeidae**			
8	Little Egret	Egretta garzetta	R/LM	Com		Sch. IV
9	Grey Heron	Ardea cinerea	R/WM	LCom		Sch. IV
10	Purple Heron	Ardea purpurea	R/LM	LCom		Sch. IV
11	Large Egret	Casmerodius albus	R/LM	LCom		Sch. IV
12	Median Egret	Mesophoyx intermedia	R/LM	LCom		Sch. IV
13	Cattle Egret	Bubulcus ibis	R/AM	Com		Sch. IV
14	Indian Pond-Heron	Ardeola grayii	R/LM	Com		Sch. IV
15	Night-Heron	Nycticorax nycticorax	R/LM	LCom		Sch. IV
	Storks	**Order- Ciconiformes**	**Family -Ciconiidae**			
16	Painted Stork	Mycteria leucocephala	R/LM	LCom	NT	Sch. IV
17	Asian Open bill-Stork	Anastomus oscitans	R/LM	LCom		Sch. IV
18	White-necked Stork	Ciconia episcopus	R	Ra		Sch. IV
	Ibises & Spoonbills	**Order-**	**Family- Threskiornithidae**			
19	Oriental White Ibis	Threskiornis melanocephalus	R/LM	LCom	NT	Sch. IV
20	Black Ibis	Pseudibis papillosa	R	UnCom		Sch. IV
21	Eurasian Spoonbill	Platalea leucorodia	R	LCom	App. II	Sch. I
	Swans, Geese & Ducks	**Order-Anseriformes**	**Family -Anatidae**			
22	Lesser Whistling-Duck	Dendrocygna javanica	R/LM	LCom		Sch. IV
23	Greylag Goose	Anser	WM	Com		Sch. IV
24	Bar-headed Goose	Anser indicus	R/WM	LCom		Sch. IV
25	Brahminy Shelduck	Tadorna ferruginea	R/WM	LCom		Sch. IV
26	Comb Duck	Sarkidiornis melanotos	R/LM	UnCom	App. II	Sch. IV
27	Cotton Teal	Nettapus coromandelianus	R/LM	LCom		Sch. IV
28	Gadwall	Anas strepera	WM	Com		Sch. IV
29	Eurasian Wigeon	Anas penelope	WM	Com		Sch. IV
30	Mallard	Anas platyrhynchos	R/WM	UnCom		Sch. IV
31	Spot-billed Duck	Anas poecilorhyncha	R/LM	Com		Sch. IV
32	Northern Shoveller	Anas clypeata	WM	Com		Sch. IV
33	Northern Pintail	Anas acuta	WM	VCom		Sch. IV
34	Garganey	Anas querquedula	WM	VCom		Sch. IV
35	Common Teal	Anas crecca	WM	VCom		Sch. IV
36	Red-crested Pochard	Rhodonessa rufina	WM	LCom		Sch. IV
37	Common Pochard	Aythya ferina	WM	LCom		Sch. IV
	Cranes	**Order-**	**Family -Gruidae**			
38	Sarus Crane	Grus antigone	R/LM	LCom	GT/Vu App. II	Sch. IV

	Rails, Crakes, Moorhens & Coots	**Order-**	**Family -Rallidae**			
39	Water Rail	Rallus aquaticus	R/WM	LCom		Sch. IV
40	White-breasted Waterhen	Amaurornis phoenicurus	R	Com		Sch. IV
41	Purple Moorhen	Porphyrio porphyrio	R/LM	LCom		Sch. IV
42	Common Moorhen	Gallinula chloropus	R/WM	Com		Sch. IV
43	Common Coot	Fulica atra	R/WM	VCom		Sch. IV
	Jacanas	**Order-**	**Family -Jacanidae**			
44	Pheasant-tailed Jacana	Hydrophasianus chirurgus	R/LM	UnCom		Sch. IV
45	Bronze-winged Jacana	Metopidius indicus	R	LCom		Sch. IV
	Painted-Snipes	**Order-**	**Family -Rostratulidae**			
46	Greater Painted-Snipe	Rostratula benghalensis	R/LM	LCom		
	Plovers & Lapwings	**Order-Charadriformes**	**Family -Charadriidae**			
47	Little Ringed Plover	Charadrius dubius	R/WM	Com		Sch. IV
48	Northern Lapwing	Vanellus vanellus	WM	LCom		Sch. IV
49	Yellow-wattled Lapwing	Vanellus malabaricus	R/LM	LCom		Sch. IV
	Sandpipers, Stints, Snipes, Godwits & Curlews	**Order- Charadriformes**	**Family -Scolopacidae**			
50	Pintail Snipe	Gallinago stenura	WM	LCom		Sch. IV
51	Common Snipe	Gallinago gallinago	R/WM	Com		Sch. IV
52	Black-tailed Godwit	Limosa limosa	WM	LCom		Sch. IV
53	Eurasian Curlew	Numenius arquata	WM	UnCom		Sch. IV
54	Spotted Redshank	Tringa erythropus	WM	LCom		Sch. IV
55	Common Redshank	Tringa totanus	R/WM	Com		Sch. IV
56	Marsh Sandpiper	Tringa stagnatilis	WM	LCom		Sch. IV
57	Common Greenshank	Tringa nebularia	WM	LCom		Sch. IV
58	Common Sandpiper	Actitis hypoleucos	R/WM	LCom		Sch. IV
59	Ruff	Philomachus pugnax	WM	LCom		Sch. IV
	Ibis , Avocets & Stilts	**Order- Charadriformes**	**Family- Recurvirostridae**			
60	Ibis	Ibidorhyncha struthersii	R/AM	UnCom		Sch. IV
61	Black-winged Stilt	Himantopus himantopus	R/LM	Com		Sch. IV
62	Pied Avocet	Recurvirostra avosetta	WM/R	LCom		Sch. IV
63	Whiskered Tern	Chlidonias hybridus	R/WM	LCom		Sch. IV

WETLAND DEPENDENT BIRDS						
Hawks, Eagles, Kites & Harriers		Order-	Family -Accipitridae			
1	Brahminy Kite	Haliastur indus	R/LM	LCom		Sch. I
2	Greater Grey-headed Fish-Eagle	Ichthyophaga ichthyaetus	R	UnCom	NT	Sch. I

ɒ

3	Western Marsh-Harrier	Circus aeruginosus	WM	LCom		Sch. I
4	Eastern Marsh-Harrier	Circus spilonotus	WM	LCom		Sch. I
5	Steppe Eagle	Aquila nipalensis	WM	LCom		Sch. I
Osprey		Order-	Family -Pandionidae			
6	Osprey	Pandion haliaetus	WM/R	UnCom		Sch. I
Falcons		Order-	Falconidae			
7	Peregrine Falcon	Falco peregrinus	R/WM	UnCom	App. I	Sch. I
Partridges		Order-	Family Phasianidae			
8	Swamp Francolin	Francolinus gularis	R	LCom	GT/Vu	Sch. IV
Owls		Order-	Family -Strigidae			
9	Brown Fish-Owl	Ketupa zeylonensis	R	UnCom	App. II	Sch. IV
10	Tawny Fish-Owl	Ketupa flavipes	R	UnCom	App. II	Sch. IV
Kingfishers		Order-Coraciiformes	Family -Alcedinidae			
11	Small Blue Kingfisher	Alcedo atthis	R/WM/	Com		Sch. IV
12	Stork-billed Kingfisher	Halcyon capensis	R	LCom		Sch. IV
13	Brown-winged Kingfisher	Halcyon amauroptera	R	LCom	NT	Sch. IV
14	White-breasted Kingfisher	Halcyon smyrnensis	R/LM	Com		Sch. IV
15	Black-capped Kingfisher	Halcyon pileata	R/LM	LCom		Sch. IV
16	Collared Kingfisher	Todiramphus chloris	R	LCom		Sch. IV
17	Greater Pied Kingfisher	Megaceryle lugubris	R	LCom		Sch. IV
18	Lesser Pied Kingfisher	Ceryle rudis	R	Com		Sch. IV
Bee-eaters		Order- Coraciiformes	Family- Meropidae			
19	Blue-cheeked Bee-eater	Merops persicus	SM/PM	LCom		
20	Blue-tailed Bee-eater	Merops philippinus	R/WM	LCom		
21	Chestnut-headed Bee-eater	Merops leschenaulti	R	LCom		
Swallows & Martins		Order-	Hirundinidae			
22	*Sand Martin	Riparia riparia	R/WM	LCom		
23	*Pale Martin	Riparia diluta	R/WM	LCom		
24	Plain Martin	Riparia paludicola	R/LM	Com		
25	Common Swallow	Hirundo rustica	R/WM	LCom		
26	Wire-tailed Swallow	Hirundo smithii	R/SM	LCom		
27	Red-rumped Swallow	Hirundo daurica	R//WM	LCom		
28	Streak-throated Swallow	Hirundo fluvicola	R/SM	LCom		
Wagtails & Pipits		Order-	Family -Motacillidae			
29	White Wagtail	Motacilla alba	R/WM/	Com		Sch. IV

6

30	Large Pied Wagtail	Motacilla maderaspatensis	R	LCom		Sch. IV
31	Citrine Wagtail	Motacilla citreola	R/WM	LCom		Sch. IV
32	Yellow Wagtail	Motacilla flava	R/WM	LCom		Sch. IV
33	Grey Wagtail	Motacilla cinerea	R/WM	LCom		Sch. IV
34	Rosy Pipit	Anthus roseatus	R/AM/WM	LCom		Sch. IV
35	*Water Pipit	Anthus spinoletta	WM	LCom		Sch. IV
Dippers		Order-	Family -Cinclidae			
36	White-throated Dipper	Cinclus cinclus	R/AM	UnCom		
37	Brown Dipper	Cinclus pallasii	R/AM	LCom		
Wrens		Order- Troglodytidae				
38	Winter Wren	Troglodytes troglodytes	R/AM	LCom		Sch. IV
Accentors		Order-	Family- Prunellidae			
39	Guldenstadt's Redstart	Phoenicurus erythrogaster	R/WM/	LCom		Sch IV
40	White-capped Redstart	Chaimarrornis leucocephalus	R/WM	Com		Sch. IV
41	Plumbeous Redstart	Rhyacornis fuliginosus	R/AM	LCom		Sch. IV
42	Little Forktail	Enicurus scouleri	R/AM	LCom		Sch. IV
43	Black-backed Forktail	Enicurus immaculatus	R	LCom		Sch. IV
44	Leschenault's Forktail	Enicurus leschenaulti	R/LM	UnCom		Sch. IV
45	Spotted Forktail	Enicurus	R/AM	LCom		Sch. IV
46	White-tailed Stonechat	Saxicola leucura	R/LM	LCom		Sch. IV
Babblers		Order-Passeriformes	Family -Timaliinae			
47	Long-tailed Prinia	Prinia burnesii	R	LCom		Sch. IV
48	Rufous-rumped Grass-Warbler	Graminicola bengalensis	R	LCom		Sch. IV

REFERENCES:

Ali, S. & S.d. Ripley (1987). Compact Handbook of The Birds of India and Pakistan Together with those of Bangladesh, Nepal, Bhutan and Sri Lanka. Oxford University Press, Delhi, 737pp.

Grimmett, R., C. Inskipp & T. Inskipp (1999). Pocket Guide to The Birds of the Indian Subcontinent. Oxford University Press, Delhi.

IUCN (2010). IUCN Red List of Threatened Species. Version 2010.4. www.iucnredlist.org. Downloaded on 01 January 2011.

Kumar, A., J.P. Sati, P.C. Tak & J.R.B. Alfred (2005). Handbook on Indian Wetland Birds and Their Conservation. Zoological Survey of India, 472pp.

Tak et al, (2003) Species richness and seasonal population changes in waterfowls. Zoological Survey of India, Fauna of Asian Wetland, Wetland Ecosystem Series 5; 43-52.

Neurochemical changes in Swiss Albino Mice brain during postnatal development

Amita Saraswat
Associate Professor, Rajrishi College,
Alwar (Rajasthan),India

Present study undertakes the neurochemical aspects of Swiss albino strain of mice during its postnatal weeks of age and body weight increased gradually throughout postnatal development. Brain to body weight increased gradually throughout postnatal development. Brain to body weight ratio and encephalization indices decreased. A sharp rise in DNA and protein concentrations has been marked which was highly significant in the growth spurt period (2-3 weeks) whereas RNA exhibited a biphasic pattern of increase with 2 peaks, on 2nd and 4th week. The highest concentration occurred on 6th week. Protein/DNA and RNA/DNA ratios were maximum on 2nd week. Acpase and ChE levels increased with advancing age whereas a raised AcPase level was seen in early postnatal interval with peak activity on 4th week.

INTROUDCTION:

Reasons for the mammalian brain as it is biochemically or otherwise relate not only to its structure and functioning but also to its origins. It is impressive to trace this development in an individual species, since it also show species specific patterns of growth during development as far as neurochemistry is concerned. The present study is focused on the various neurochemical parameters, DNA, RNA protein and enzymes like AlPase, AcPase and ChE in the postnatally developing mouse brain. Besides body and brain weights, their ratios and encephalization index, which is measure for estimation of neural variables such as cortex size, number of neurons and the average neuronal density, have also been taken into account. These observations were recorded on 1,2,3,4,5 and 6th week of age.

MATERIALS AND METHODS:

Mice at 1,2,3,4,5 and 6 weeks of age were sacrificed by cervical dislocation, their brains were removed and whole brain homogenates were prepared as suggested in methods proposed by Fiske and Subbarow

(1) for acid and alkaline phosphates, Ceriotti (2) for deoxyribase and ribose nucleic acids, Lowry et al (3) for protein and Huerga et al

(4) for cholinesterase estimations. These homogenates have been estimated calorimetrically following these methods. Encephalization index (c) has been worked out by formula given by Hofman (5).

RESULTS:

Figure depicts the changes in the body and brain weights of one to six weeks old mice plotted as percentage of weights of six weeks old mice.

It shows that body weight increased gradually form 1st (30.34%) to 6th

(100%) week parturition, which were highly significant ($P<0.001$) on first, second and third week. The brain weights too showed a sharp increase from 1 week to 2 week old mice. Brain to body weight ratio decreased with advancing age. Calculated as percentage of ratio at 6th week. It decreased to one third of its value at first week. At maturity the encephalization index showed a decline to just half of its value at the 1st week .

During postnatal growth of brain the deoxyribonucleic acid content of the cell increased continuously. However, between 2 to 3 weeks of age, which is regarded as 'growth spurt period', it decreased by 25%

($P<0.01$) protein concentration in one week old mice (58.37%) showed a sharp rise to 93.38% at the 3rd week. Between 2nd and 3rd week, an increase by 16.68% has been recorded.

However, later on the increase became only 3.88, 0.66 or 2.18% between consecutive weeks (Table-I)

The ribonucleic acid concentration showed biphasic pattern with 2 peak one on 2nd and another on 4th week, highest at 4 week (173.78%) post partum. The changes were non-significant throughout the observation span except at the 4th week. Protein/DNA ratio increased in 1st week

(106.12%) and showed a peak at the 2nd week (122.68%) post partum.

RNA/DNA ratio too was found to increase during the last week (187.36%) and at 2 weeks (201%) of age. But could not maintain such a high level and declined on 3rd week (184%) and showed another peak at the 4th week . Cell index which denotes the number of cells in a unit measure of tissues showed an increase in the same proportion as seen in DNA concentrations with the advancing age. An increase by about 50% has been noticed form 1 week of age onward. Between 2 and 3 weeks the maximum gain , 4/6 the value at 6 week of age was recorded .

Enzymes:

Acid phosphates showed a gradual decline till 5 weeks(73.49%) post partum ; the adult value is gained by a sharp rise (26.51%) at 6 weeks of age. Alkaline phosphates activity follows an altogether different course. Thus, it showed an increased value in early postnatal period with a peak at the 4th week. The changes were non-significant at 1st, 4th and 5th weeks post partum, whereas the increase was significant at the 2nd ($P<0.001$) and 3rd ($P<0.01$) weeks.

Cholinesterase, an enzyme of physiologically immense importance in brain function, is found to increase in concordance with the increase in brain weight although to an extent lesser by approximately 20%. However, the increase followed a pattern similar to that of brain weight.

DISCUSSION:

Observations indicate that body and brain weights gained significant rise in 1 to 3 weeks of ages as compared to late postnatal age groups (Fig1).

The size of the brain in relation to body weight becomes smaller with advancing age. This significant increase in brain and body weights can be a result of rapid multiplication of cells in first fortnight after birth. Similar increase was reported in little pocket mouse (Perognathus longimembus) during its postnatal development. About 65% of the adult weight (8-10gms) was attained in 2 days. Semilogaritmic plots of ear, hindfoot, tail and fetal body length and weight showed polyphonic growth with initial instantaneous growth rates 9. In 1 week old mice it was 20% if the weight at 6th week of age (Fig.1) ,But the brain weight gain was only 35% during postnatal growth i.e. 1-6 weeks of age. The cell index (measure of cell number) too showed a 45% increase during this period.

Himwich (6) also reports that in the case of postnatal rats, the actual brain weight gain (less than 1.5gm) from birth to maturity is negligible compared to the body weight over the same period (several hundred grams) . In brain, as in other tissues, the nucleic acids provide for the storage and transmission of genetic information as well as translation of this information into the synthesis of cellular proteins. Such processes are obviously involved in the way information is handled in gestational periods of growth. An increase in DNA is an indication of cell proliferation in the rat upto10 days of age (7).Thus, the observed (Table1) increase in DNA may be due to active cell proliferation . But another report in rate states that, in less than 3 weeks' time maximum accumulation of DNA takes place after that , the curve (age vs concentration) levels off (8). The total amount of brain DNA reaches adult levels quite early in developmen , about 14 days in the rat (9) whereas RNA content is somewhat slower to reach a maximum , 30 days in the rat (10). Studies are in good conformity with our observation (Table 1) Changes in the quantity of RNA (Ribonucleic acid) during development follows a characteristically different course from that of deoxy-compound (9). Its content per unit of DNA (i.e. cell) changes from about 0.5 at 25 days gestation to over 3 in adult. These ratios are common to many species and to most but not all tissue(11). The RNA in the transcription of genetic information (mRNA) as components of ribosome's (RNA) and as an intermediate in the activation of amino acids (acyl t-RNA) is responsible for active synthesis of new proteins during fetal and postnatal development . Although new protein synthesis ceases at maturation,

RNA synthesis continues at a diminished rate and a rapid turnover persists throughout the life span of the organs. In the brain of the fetal rat and in the early postnatal period the formation of new glial elements and the extension of axons as well as the proliferation of dendrite processes, reflect the continuous and active formation of RNA and other cell constituents (12).

In mouse brain, the total protein was high at birth, exhibited a slight fall until seven days of age and then increase with age by a factor of 1.6 reaching the adult level by the thirtieth day of postnatal life(13). The same holds true with our observations, since at 4 week (28 days) protein concentration was 97% of sixth week's concentration (Table 1) Davison and Dobbing (14) also maintained that the protein content of the brain increase with age from 5 per cent at birth to 10 per cent of the wet weight in the 30-day–old rat .

Thereafter, there is an increase in the absolute content of brain protein ending at about 50 days of age after which the brain weight increases only slowly. Developmental increase in the protein contents of the rat brain has been found to occur concomitantly with the appearance of myelin and with the morphological differentiation of the CNS (15). The critical period for the deposition of protein for mouse and rat brain appeared to be between ten and thirty days of postnatal age (16,17). In the present study protein content , from 58% at seven day reached 98% (of concentration at sixth week) on 35th day after birth (Fig.1) Bayer and Mc Murray(9) observed that the protein concentration in the rat brain doubled between birth and maturity using from 5.5 to 9.5 per cent of the wet weights. Pitts and Quick

(18) by means of taking brain samples every day have demonstrated a phenomenal increase in total protein of rat brain at tenth day. This spurt followed by quiescent period during which there was little change in total protein. In our study also we observe from first, second and third weeks there was 19 to 16 % increase as compared to 7 or 0.6 or 2% increase on other periods (Table1) . The later periods can be regarded as quiescent periods. According to Timers (20) also the rate of protein synthesis is highest during development and decreases significantly when the animals reach adulthood.

Characteristic changes occur in the mean chemical composition of cells in the brain during development. There is an increase in alkaline phosphates level from 1st to 3rd week and then it decreased continuously to show an overall decline by 29%.

In neural tissues from embryos of chick and man, alkaline phosphates wasparticularly high and diminished during development (19). According to Timers (20) also unlike the may enzymes that appear during development and increase towards adulthood, AlPase show a high activity in the early fetal phases of brain development with a decrease toward adulthood ; on the contrary, acid phosphates activity declined from 92% to 74% till 5thweek then suddenly increased by 26% .

Thus, AcPase showed an overall increase by 8% in (1-6 weeks of postnatal life). A number of reports indicate that acid phosphates, continues to increase during postnatal development. In human fetal brain the earliest differentiated nerve cells too show phosphates activity in Purkinje cells. Cholinesterase (ChE) activity increased by about 50% between 1 to 6 weeks of age (Table1) . Neural tissues show relatively high ChE activity from an early stage of development.

Cholinesterase is predominantly localized in blood vessels and in glial cells where it has been thought to play a role in metabolism of myelin. Activity of ChE in humans and rats shows increase when the cerebral cortex is only in the beginning phase of increasing activity. Differences were exhibited between different strains of rat; and also by using different substrates. Several esterases hydrolyzing naphthylacetylate and homologous were shown to develop in the brain during first 30 days of rat (6).

ACKNOWLEDEMENT:

The authors are grateful to CSIR,New Delhi for financial assistance.

REFERENCES:

1. Fiske, C.H. and Subbarow,Y 1925 'The colorimetric determination of phosphorus', J. BiolChem , 66 , 375-400.
2. Ceriotti, G. 1955 'Determination of nucleic acid in animal tissue' .J. Biol Chem., 214,59-70.

3. Lowry O.H. RosenbroughN.J . Farr A. and Randall ., R.J. 1951'Protein measurement with folin – phenol reagent', J. Biol . Chem., 193, 265-275.
4. Huerga , J. de La, Yesinick , Ch, and popper , H, Amer J. Chin Path 1952, 22 ,1126
5. Hofman , M.A. 1982, 'A two component theory of encephalization in mammals' . J. Theory ,Biol ,99 , 571-584
6. Himwich ,W. 1962, 'Biochemical and neurophysiological development of the brain in neonatal period'.Intl. Rev. Neurobiol 4 ,117-158
7. Winick, M, and Noble, A ,1965, 'Qualitative changes in DNA , RNA nd protein during prenatal and postnatal growth in rat', Develop.Biol.12 ,451-466
8. Dhopeshwarkar, G.C.,1983, 'Nutrition and Brain Development' Plenium Press, New York and London , pp 19-21
9. Bayer, S.M. and Mc Murray. W.C. 1967, 'The metabolism of amino acids in developing rat brain' . J. Neurochem. 14 ,695-706
10. Mcllwain ,H, and Bachelard H,S, 1971, 'Biochemistry and the Central Nervous System Churchill Livingstone, Edinburg and London , pp 402-415
11. Oja, S,S, 1956, Studies on protein metabolism in developing rat brain Ann. Acad, Sci, Fenn, (Med.) 131 ,7-81.
12. Brizzee, K.R., 1964, 'Effects of single and fractionated doses of total body X- irradiation in utero on growth of the brain and its parts' ,Nature , 202,262-264
13. Himwich ,W. 1973, 'Early studies of the developing brain' Biochemistry in Brain Research , Marcel Dekkar, New York 1, 1-53.
14. Hayden , P. and Gambino , J.J. 1966, 'Growth and development of the little pocket mouse Perognathus longimembris' , Growth 30, 187-197
15. Davison , A.N. and Dobbings, 1969 J.Neurochemistry , Blackwell Scientific publications, Oxford and Edinburg , p 277
16. Folch, Pi.,1955 'Composition of the brain in relation to maturation' H. Woctsch (Ed) Biochemistry of Development of Nervous System , Academic Press, new York , pp 121-133
17. Clouet , D.H. and Gaitonde , M.K. 1956, 'The changes with age in the protein composition of rat brain' .J. Neurochem. 1 ,126-133
18. Pitts, F,N. Jr. and Quick C.,1967,'Brain succinate semialdehyde dehydrogenase II. Changes in the development rat brain' . J. Neurochemi .,14,561-570
19. Cohen, S.R.1970, Handbook of Neurochemistry , 3, 87
20. Timiras, P.S., 1972, 'Developmental physiology and Aging', The MacMillan Co., New York and Collier- MacMillan Ltd., London, p 387

Comparative Study of Brassica juncea Stem and Dry leaves Powder as Anticorrosive Biomaterial

Jyoti Sharma , Sushmita
[1]Associate Professor, Department of Chemistry, Raj Rishi College Alwar (Raj.)
[2]Research Scholar, Department of Chemistry, RRBM university Alwar (Raj.)
E-mail: sharma_ak002@yahoo.com

Abstract: Corrosion inhibition characteristics of dry leaves powder and stem powder of Brassica juncea plant has been investigated on Aluminium metal in 1N HCl solution. The study was carried out using gravimetric analysis. The analysis of result showed that inhibition efficiency increases with increase in concentration of both leaves powder and stem powder in acidic solution. The efficiency of leaf powder (70%) was found to be more as compared to the stem powder (55%). The Brassica juncea plant is grown in wide area and its dry parts are easily available after harvesting. The above-mentioned biomaterial is ecofriendly, low-cost and easily available.

Key words: Corrosion inhibitor, low-cost, biomaterial.

1. INTRODUCTION

Industrial application such as industrial cleaning and processing of oil wells have great importance of metal and alloy container. To reduce corrosion of metal many chemical inhibitors has been used which are toxic and expensive, so the researchers have interest of using alternative of toxic chemical inhibitors and the search for non-toxic natural inhibitors. Corrosion caused by acid solutions such as acid pickling and acid descaling to metal can be prevented by using inhibitors. Research towards formulation of safe inhibitor, plant extract has become ecofriendly, economical and readily available source of effective corrosion inhibitor. Inhibition characteristics of different green inhibitors have been studied. However, there is still a need of research on other plants as inhibitor in industrial application.

In this paper we have used waste part of brassica juncea plant to find corrosion inhibition efficiency for aluminium metal strips. Since Brassica Juncea is grown in abundance over the world with common name of mustard and available at relatively cheaper rate. Dry waste part of mustard plant is easily available in fields. The objective of this study was to investigate the inhibitory effect of dry leaves powder and stem powder of Brassica juncea for Aluminium metal in 1N HCl solution.

2. MATERIALS AND METHODS

2.1 Materials

Aluminium coupons of dimensions 5cm x 2cm x 0.1 cm have been used for this study. Aluminium samples were pre-treated before the test by cleaning with emery paper, cleaned with distilled water and acetone, dried at room temperature before use. 1 N hydrochloric acid was prepared by dilution of analytical grade 37% HCl with deionized water.

2.2 Preparation of Leaves and Stem Powder

Brassica juncea plants were collected from fields of Satnali, Haryana (India) in March 2019. The green leaves and stem part were dried in an open room for a period of one month. After 30 days the leaves were powdered with the help of pestle and mortar, stems were powdered in flour mill at home and stored in closed container for experimental work.

Fig1.Collection and Preparation of Leaves Powder of Brassica juncea Plant

2.3 Weight Loss Measurement

For weight loss measurement, aluminium specimens of 5cm x 2cm x 0.1 cm sizes were pretreated and weighed accurately using an analytical balance before each immersion; the aluminium coupons were immersed in 100 ml capacity beakers containing 40 ml of hydrochloric acid in the absence and presence of various concentrations of leaves and stem powder of Brassica juncea. Triplicate specimens were immersed in acidic solution for 24 hours in the absence and presence of 1g, 2g, 3g, and 4g of leaves powder and stem powder. After immersion period (24h), the aluminium sample were withdrawn, prudently washed with distilled water, ultrasonic cleaning in acetone, dried at room temperature and then weighed. Each experiment was repeated three times and the mean value was calculated. From the weight loss data obtained, the corrosion rates (CR), inhibition efficiency (IE) and surface coverage (Θ) were calculated using equations (i) – (iii) respectively:

$$CR = \frac{\Delta W}{AT} \qquad \text{(i)}$$

where, ΔW is weight loss, A is the area of the coupon in cm^2 and T is time in hour. CR^{inh}

$$IE\% = \left(1 - \frac{\quad}{CRblank}\right) \times 100 \qquad \text{(ii)}$$

where CRinh and CRblank correspond to the corrosion rates in the blank and inhibitor solutions respectively, and the surface coverage was calculated using CR^{inh}

$$\theta = \left(1 - \frac{\quad}{CRblank}\right) \qquad \text{(iii)}$$

3. RESULT

3.1 Phytochemical Screening

Brassica juncea contain glucosinolate. The presence of this compound has been reported to promote corrosion inhibition in acidic media. Structure of glucosinolate as shown in Fig.2

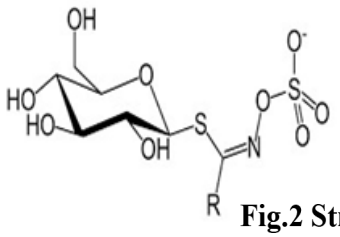

Fig.2 Structure of Glucosinolate

3.2 Mass loss Measurement

The variation in mass loss of aluminium in 1N HCl solution in the presence of the different concentrations of leaves powder and stem powder of mustard plant for 24 hours at 298 K has been represented in fig 3. It is clear that corrosion rate decrease and inhibition efficiency increase with increase in concentration of leaves and stem powder. Mass loss of aluminium metal in 1N HCl solution is less as we increase the leaves powder concentration. Mass loss of aluminium in blank solution is 0.3g and in leaves powder inhibitor solution is 0.1g. Decrease in mass loss of aluminium metal is more as we increase the concentration of leaf powder (3.5g) in comparison to the mass loss in the presence of stem powder (4g). Adsorption on the metal surface creates a barrier for charge and mass transfer leading to a decrease in the interaction between the metal and the corrosive environment. Due to adsorption of powder on metal surface, less surface area of metal was in contact of acid solutions and mass loss of aluminium metal becomes less. This shows that adsorption of powder on metal surface reduces the oxidation of metal.

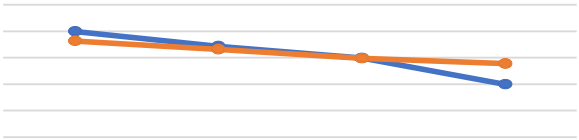

3.3 Comparative result

The variation of inhibition efficiency (IE%) with concentration of leaves powder and stem powder in HCl solution has been represented in fig 4. From the figure it is observed that inhibition efficiency of leaves powder is more than stem powder. The inhibition efficiency increases with increase in leaves powder, varying from 46% to 70% in the concentration range of 1 to 4g and inhibition efficiency of stem powder vary from 42% to 55%. It was found that inhibition efficiency decreases with increase in temperature.

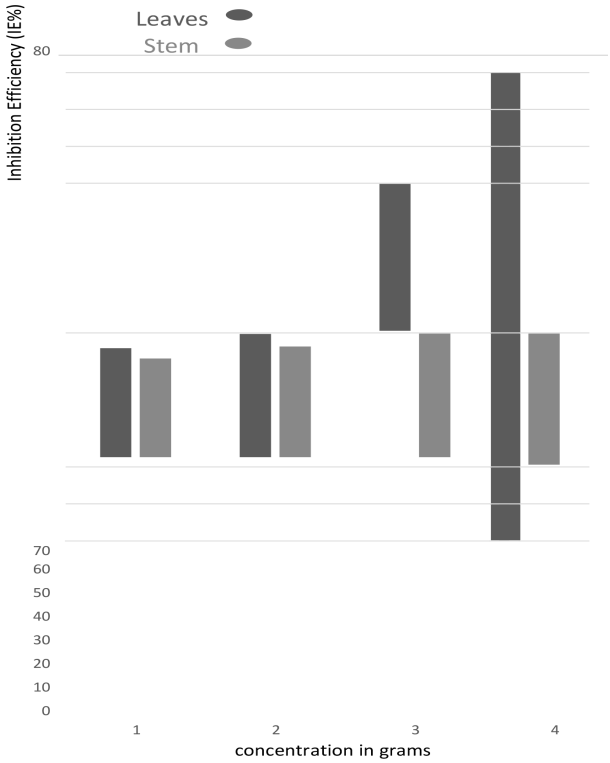

4. CONCLUSION

This study investigated the properties of corrosion inhibition of leaves and stem powder of Brassica juncea plant on aluminium in 1 N HCl using the conventional gravimetric measurements. The analyses of the results showed that the inhibition efficiency was acid solutions. The efficiency of leaves powder (70%) was found to be more in comparison increased with increase in concentration of the inhibitor but decreased with temperature in to stem powder (55%).

5. REFERENCES

1. Alaneme, K. (2015). Corrosion Inhibition and Adsorption Characteristics of Rice Husk Extracts on Mild Steel Immersed in 1M H2SO4 and HCl Solutions. *International Journal of Electrochemical Science*, 10, 3553-3567.
2. Al-Senani G.M., A. M. (2018). Study the Corrosion Inhibition of Carbon Steel in 1 M HCl Using Extracts of Date Palm Waste. *Int. J. Electrochem. Sci*., 13, 37773788.
3. Ferreira K.C.R., C. N. (2016). Corrosion Inhibition of Carbon Steel in HCl Solution by Aqueous Brown Onion Peel Extract. *Int. J. Electrochem. Sci*., 11, 406-418.
4. Ali I.H., (2016). Inhibitory Effect of Leaf Extract of Khaya senegalensis (Mahogany) on C-steel Corrosion in 1.0 M Hydrochloric Acid Solution. *Int. J. Electrochem. Sci*.,11, 2130-2141.
5. Tomic M.V., V.M. (2016). Sage Extracts as Inhibitors of Steel Corrosion in 4% HCl. *Int. J. Electrochem. Sci*., 11, 3339-3350.
6. Al-Senani G.M., A. M. (2018). Study the Corrosion Inhibition of Carbon Steel in 1 M HCl Using Extracts of Date Palm Waste. *Int. J. Electrochem. Sci*., 13, 37773788.
7. Guo Y., G. M. (2017). Tobacco Rob Extract as Green Corrosion Inhibitor for N80 Steel in HCl Solution. *Int. J. Electrochem. Sci.*, 12, 1401-1420.
8. Salghi R., J. S. (2017). Inhibition of C-steel Corrosion by Green Tea Extract in Hydrochloric Solution. *Int. J. Electrochem. Sci.*, 3283-3295.
9. Zheng X., G. M. (2017). Corrosion Inhibition of Mild Steel in Sulfuric Acid Solution by Houttuynia Cordata Extract. *Int. J. Electrochem. Sci.*, 12, 62326244.

Role of Zinc Oxide as a Photocatalyst in Photo-Bleaching of Basic Fuchsin

Seema Gulati, Ritu Mathur

Department of Chemistry, R.R. College, Alwar (India)

Abstract: The photocatalytic bleaching of basic fuchsin over zinc oxide has been carried out. The effects of various parameters such as pH, concentration of basic fuchsin, amount of semiconductor and light intensity have been observed and a tentative mechanism has been proposed.

Keyword: Photocatalytic bleaching, Dye, Zinc oxide, Basic fuchsin, semiconductor.

V. Homen and L. Santos[1] have studied the degradation and removal method of Antibiotics from Aqueous Matrices. K. Nakata and A.Fujishima[2] have stated Design and Applications of TiO_2 photocatalysis. L.Rizzo, S. Meric, M.Guida, D. Kassinos, V. Begiorno[3] carried out heterogeneous photocatalytic degradation kinetics and detoxification of urban wastewater treatment plant effluent contaminated with pharmaceuticals. Somani et al.[4] used some charge transfer complex forming dyes incorporated in solid polymer electrolyte for optical humidity sensing. Wang et al.[5] used metallized thiazolylazo dyes as optical recording materials, while Je et al.[6] have also used hemicyanine dye for this purpose. Chen et al.[7] have reported preparation of Nb_2O_5 coated TiO_2 nanoporous electrodes and their applications in dye sensitized solar cells.

Inspite of many uses, the dyes are toxic and carcinogenic in nature and environmental contamination by these toxic chemicals is emerging as a serious global problem. Coloured solutions containing dyes from industrial effluents of textile, dyeing and printing industries may cause skin cancer due to photosensitization and photodynamic damage. On the contrary, bleached dye solution is less toxic and almost harmless. Secondly, dye containing coloured water is of almost no use, but if this coloured solution is bleached to give colourless water, then it may be used for washing, cooling, irrigation and cleaning purpose. Thus, photocatalytic bleaching will provide a low cost method to solve this problem.

Results and Discussion: The photocatalytic bleaching of Basic fuchsion (BF) was observed at λ_{max} 540 mm. The results for a typical run is given in Table 1 and graphically represented in Fig. 1.

The plot of O.D. v/s time was linear but in two stages; the first stage being faster. Hence, both the stages of this reaction follow pseudo-first order kinetics. The rate constants of this reaction were determined by expression 1. Rate constant (k) = 2.303 x slope. (Expression 1)

Table 1

A TYPICAL RUN

[Basic Fuchsin] = 1.5 x 10^{-5} M, pH = 5.5, Light Intensity = 40.0 mW cm^{-2}, Zinc oxide = 0.10 g.

Time (Min.)	Optical Density (O.D.)	1+log (O.D.)
0..0	0.715	0.854
30.0	0.603	0.780
60.0	0.502	0.700
90.0	0.473	0.674
120.0	0.452	0.655
150.0	0.437	0.640
180.0	0.425	0.628
210.0	0.412	0.614

$k_1 = 9.30 \times 10^{-5}\ s^{-1}$

$k_2 = 1.94 \times 10^{-5}\ s^{-1}$

Effect of pH : The effect of pH on the rate of bleaching of BF was investigated in the pH range (pH = 5.0 to 7.5). The semiconductor zinc oxide was dissolved in presence of highly acidic media and, therefore, photocatalytic bleaching could not be investigated in lower pH range. It was observed that dye solution was decolourised at higher pH values. The results are reported in Table 2.

Table 2

Effect of pH

[Basic Fuchsin] = 1.5 x 10-5 M, Light Intensity = 40.0 mW cm-2, Zinc Oxide = 0.10 g.

pH	Rate Constant (s^{-1})	
	$k_1 \times 10^5$	$k_2 \times 10^5$
5.0	8.50	1.37
5.5	9.30	1.94
6.0	7.88	1.77
6.5	7.53	1.61
7.0	7.20	1.50
7.5	6.95	1.44

It was observed that with increase in the pH of medium, the rate of photocatalytic bleaching of basic fuchsin increases up to pH 5.5. A further increase in pH value of the reaction mixture affects the rate of photocatalytic bleaching adversely. This may be explained on the basic that at lower pH values, there will be an electrostatic attraction between cationic dye and the surface of the semiconductor, which is electron rich due to presence of adsorbed OH^- ions. But after certain value of pH i.e. 5.5, a further increase in pH will make semiconductor surface positively charged due to the adsorption of H^+ ion on its surface. In this situation, the approach of cationic dye molecules towards the semiconductor surface will face an electrostatic repulsion and, therefore, the rate of photocatalytic bleaching will decrease again.

Effects of basic fuchsin concentration: Effect of variation of dye concentration was also studied by taking different concentrations of basic fuchsin. The results are tabulated in Table 3.

Table 3

Effect of basic fuchsin concentration

pH = 5.5, Zinc oxide = 0.10 g, Light Intensity = 40.0 mW cm^{-2}

[Basic Fuchsin] x 10^5 M	Rate Constant (s^{-1})	
	$k_1 \times 10^5$	$k_2 \times 10^5$
0.5	3.50	1.54
1.0	4.81	1.81
1.5	9.30	1.94
2.0	8.59	2.44
2.5	7.82	1.73
3.0	5.15	1.30

It has been observed that the rate of photocatalytic bleaching increases with an increase in the concentration of the dye. It may be due to the fact that as the concentration of basic fuchsin was increased,

more dye molecules were available for excitation and energy transfer and hence, an increase in the rate was observed. The rate of photocatalytic bleaching was found to decrease with an increase in the concentration of the dye, further. This may be attributed to the fact that the dye will start acting as a filter for the incident light and it will not permit the desired light intensity to reach the semiconductor particles; thus, decreasing the rate of photocatalytic bleaching of basic fuchsin.

Effect of amount of semiconductor: The effect of amount of semiconductor on the rate of photocatalytic degradation of BF was also observed by taking different amounts of semiconductor. The results are reported in Table 4.

Table 4

Effect of Amount of Semiconductor

[Basic Fuchsin] = 1.5 x 10^{-5} M, pH = 5.5, Light Intensity = 40.0 mW cm^{-2}

Amount of Semiconductor (g)	Rate Constant (s^{-1}) k_1 x 10^5	k_2 x 10^5
0.02	5.48	1.04
0.04	6.20	1.10
0.06	6.96	1.28
0.08	8.21	1.60
0.12	9.29	1.95
0.14	9.30	1.94

It has been observed that the rate of photobleaching of basic fuchsin increases with an increase in the amount of semiconductor but ultimately, it becomes almost constant after a certain amount. This may be due to the fact that as the amount of semiconductor was increased, the exposed surface area also increases, but after a certain limit, if the amount of semiconductor was further increased; there will be no increase in the exposed surface area of the photocatalyst. It may be considered like a saturation point; above which, any increase in the amount of semiconductor has negligible or no effect on the rate of photocatalytic bleaching of basic fuchsin. As any increase in the amount of semiconductor after this saturation point will only increase the thickness of the layer at the bottom of the vessel, once the complete bottom of the reaction vessel is covered by the photocatalyst.

It may be also confirmed on the basis of geometry of the reaction vessel. This was observed by taking reaction vessels of different dimensions. The point of saturation was shifted to higher value, when vessels of larger capacities were used. A reverse trend was observed, when vessels of smaller capacities were used.

Effect of light intensity: The effect of light intensity on the photocatalytic degradation of BF was also observed. The results are summarized in Table 5.

Table 5

Effect of Light Intensity

[Basic Fuchsin] = 1.5 x 10^{-5} M, Zinc oxide = 0.10 g, pH = 5.5

Intensity of light (mW cm^{-2})	Rate Constant (s^{-1}) k_1 x 10^5	k_2 x 10^5
20.0	7.78	1.78
30.0	8.70	1.88
40.0	9.30	1.94
50.0	10.23	2.25
60.0	10.96	2.70
70.0	11.51	2.83

The results given in Table 5 indicate that bleaching action was accelerated as the intensity of light was increased because any increase in the light intensity will increase the number of photons striking per unit area of semiconductor powder. A linear behavior between light intensity and rate of reaction was observed.

Mechanism: On the basis of these observations, a tentative mechanism for photocatalytic bleaching of basic fuchsin may be proposed.

^1BF hv ^1BF ..... 1 $\xrightarrow{}$ 01

$^1BF_1$ $\longrightarrow$ ISC $^3BF_1$ 2

$^3BF_1$ + ZnO BF^+ + $\longrightarrow$ ZnO (e^-) 3

ZnO (e^-) + O_2 ZnO $\longrightarrow$ + O_2^* 4

$\longrightarrow$ H^+ + O_2^* $HO_2^\bullet$ 5

$HO_2^\bullet$ + BF^+ BFH + $\longrightarrow$ O_2 6

When the solution of basic fuchsin (BF) was exposed to light in presence of semiconductor; initially the dye molecules are excited to first excited singlet state. Then these excited singlet molecules are transferred to triplet state through intersystem crossing (ISC). The triplet dye may donate its electron to the semiconductor and the basic fuchsin becomes positively charged. The dissolved oxygen of solution will pull an electron from conduction band of semiconductor; thus
regenerating semiconductor and O_2^* is formed. In acidic medium, oxygen ion radical reacts with proton to form HO_2^* radical. This radical reduces the positively charged basic fuchsin (BF) molecules in leuco (BFH), regenerating oxygen molecules. The participation of HO_2^* radicals as an active species was confirmed by carrying out the reaction in presence of HO_2^* ion scavenger e.g. 2propanol, where the reaction rate was drastically retarded.

EXPERIMENTAL

Basic Fuchsion (s.d. fine) and zinc oxide (C.D.H.) were used in the present investigations. The dye solution of basic fuchsin (BF) was prepared in doubly distilled water. The photocatalytic bleaching of BF was studied in the presence of semiconducting zinc oxide and light. 0.0338 g of BF was dissolved in 100.0 ml. of doubly distilled water so that the concentration of the dye solution was 1.0 x 10^{-3} M. It was used as a stock solution. The photocatalytic bleaching of BF was observed taking 200.0 ml. of dye solution (1.0 x 10^{-5} M.) and 0.10 g of zinc oxide semiconductor. A 200 W tungsten lamp (light intensity 40.0 mW Cm^{-2}) was used for irradiating the reaction mixture in the visible range. The intensity of light at various distances from the lamp was measured with the help of a solarimeter (Surya Mapi Model CEL 201). A water filter was used to cut off thermal radiations. The pH of the solution was measured by a digital pH meter (Hanna instruments ISO-9001). The desired pH of the solution was adjusted by the addition of previously standardized sulphuric acid and sodium hydroxide solution. A UV spectrophotometer (Systronics Model 108) was used for measuring absorption maximum and optical density (O.D.) at different time intervals.

REFERENCES

1. V. Homen and L. Santos, Degradation and Removal of Antibiotics from Aqueous Matrices – A Review, J. Environ. Manag., **92**, 2304-2347 (2011).
2. K. Nakata and A. Fujishima, TiO_2 Photocatalysis : Design and Applications, J. Photochem. Photobiol.C,**13**, 169-189 (2012)
3. L.Rizzo, S. Meric, M.Guida, D. Kassinos, V. Begiorno, Heterogeneous Photocatalytic Degradation Kinetics and Detoxification of an Urban Wastewater Treatment Plant Effluent Contaminated with Pharmaceuticals, Water Research, **43**, 4070-4078 (2009).
4. P.R. Somani, A.K. Viswanath, R.C. Aiyer and S. Radhakrishan 2001, Sensor, Actuator, **80B**, 141

(2001).
5. S.Q. Wang, S.Y. Shen, H.J. Xu, D.H. Gu, J.L. Yim and X.Y. Dong, Mater. Sci. and Eng. **79B**, 45 (2001).
6. J.T. Je, K.Y. Lee and K.S. Min., Mol. Cryst. Liq. Cryst., **371**, 233 (2001).
7. S.G. Chen, S. Chappel, Y. Diamant and A. Zaban, Chem. Mater., **12**, 4629 (2001).

Heavy Metals: Sources, Effect on plants and their phytoremediation treatment

Jagat Pal Singh
Department of botany
Govt. college, Deeg (Rajasthan), INDIA

Abstract
Heavy metals are among the most important sorts of contaminant in the environment. Several methods already used to clean up the environment from these kinds of contaminants, but most of them are costly and difficult to get optimum results. Currently, phytoremediation is an effective and affordable technological solution used to extract or remove inactive metals and metal pollutants from contaminated soil and water. This technology is environmental friendly and potentially cost effective. This paper aims to compile some information about heavy metals of arsenic, lead, and mercury (As, Pb, and Hg) sources, effects and their treatment. It also reviews deeply about the heavy metal uptake mechanisms and several research studies associated about the topics.

Introduction

Heavy metals are among the contaminants in the environment. Beside the natural activities, almost all human activities also have potential contribution to produce heavy metals as side effects. Migration of these contaminants into noncontaminated areas as dust or leachates through the soil and spreading of heavy metals containing sewage sludge are a few examples of events contributing towards contamination of the ecosystems.

Several methods are already being used to clean up the environment from these kinds of contaminants, but most of them are costly and far away from their optimum ;chemical and thermal methods are both technically difficult and expensive that all of these methods can also degrade the valuable component of soils. Conventionally, remediation of heavy-metal-contaminated soils involves either onsite management or excavation and subsequent disposal to a landfill site. This method of disposal solely shifts the contamination problem elsewhere along with the hazards associated with transportation of contaminated soil and migration of contaminants from landfill into an adjacent environment. Soil washing for removing contaminated soil is an alternative way to excavation and disposal to landfill. This method is very costy and produces a residue rich in heavy metals, which will require further treatment. Moreover, these physio-chemical technologies used for soil remediation render the land usage as a medium for plant growth, as they remove all biological activities.

Recent concerns regarding the environmental contamination have initiated the development of appropriate technologies to assess the presence and mobility of metals in soil , water, and wastewater. Presently, phytoremediation has become an effective and affordable technological solution used to extract or remove inactive metals and metal pollutants from contaminated soil. Phytoremediation is the use of plants to clean up a contamination from soils, sediments, and water. This technology is environmental friendly and potentially cost effective. Plants with exceptional metal-accumulating capacity are known as hyperaccumulator plants. Phytoremediation takes the advantage of the unique and selective uptake capabilities of plant root systems, together with the translocation, bioaccumulation, and contaminant degradation abilities of the entire plant body.

Many species of plants have been successful in absorbing contaminants such as lead, cadmium, chromium, arsenic, and various radionuclides from soils. One of phytoremediation categories, phytoextraction, can be used to remove heavy metals from soil using its ability to uptake metals which are essential for plant growth (Fe, Mn, Zn, Cu, Mg, Mo, and Ni). Some metals with unknown biological function (Cd, Cr, Pb, Co, Ag, Se, Hg) can also be accumulated [5].

The objectives of this paper are to discuss to provide a brief view about heavy metals uptake mechanisms by plant, to give some description about the performance of several types of plants to uptake heavy metals and to describe about the fate of heavy metals in plant tissue, especially on arsenic (As), lead (Pb), and mercury (Hg).

Heavy Metals: Sources and Effect in the Environment

Heavy metals are conventionally defined as elements with metallic properties and an atomic number >20. The most common heavy metal contaminants are Cd, Cr, Cu, Hg, Pb, and Zn. Metals are natural components in soil [6]. Some of these metals are micronutrients necessary for plant growth, such as Zn, Cu, Mn, Ni, and Co, while others have unknown biological function, such as Cd, Pb, and Hg.

Metal pollution has harmful effect on biological systems and does not undergo biodegradation. Toxic heavy metals such as Pb, Co, Cd can be differentiated from other pollutants, since they cannot be biodegraded but can be accumulated in living organisms, thus causing various diseases and disorders even in relatively lower concentrations. Heavy metals, with soil residence times of thousands of years, pose numerous health dangers to higher organisms. They are also known to have effect on plant growth, ground cover and have a negative impact on soil microflora [8]. It is well known that heavy metals cannot be chemically degraded and need to be physically removed or be transformed into nontoxic compounds.

Mechanisms of Heavy Metal Uptake by Plant

Contaminant uptake by plants and its mechanisms have been being explored by several researchers. It could be used to optimize the factors to improve the performance of plant uptake. According to Sinha et al. ,the plants act both as “accumulators” and “excluders”. Accumulators survive despite concentrating contaminants in their aerial tissues. They biodegrade or biotransform the contaminants into inert forms in their tissues. The excluders restrict contaminant uptake into their biomass.

Plants have evolved highly specific and very efficient mechanisms to obtain essential micronutrients from the environment, even when present at low ppm levels. Plant roots, aided by plant-produced chelating agents and plant-induced pH changes and redox reactions, are able to solubilize and take up micronutrients from very low levels in the soil, even from nearly insoluble precipitates. Plants have also evolved highly specific mechanisms to translocate and store micronutrients. These same mechanisms are also involved in the uptake, translocation, and storage of toxic elements, whose chemical properties simulate those of essential elements. Thus, micronutrient uptake mechanisms are of great interest to phytoremediation.

The range of known transport mechanisms or specialized proteins embedded in the plant cell plasma membrane involved in ion uptake and translocation include (1) proton pumps (″-ATPases that consume energy and generate electrochemical gradients), (2) co- and antitransporters (proteins that use the electrochemical gradients generated by ″-ATPases to drive the active uptake of ions), and (3) channels (proteins that facilitate the transport of ions into the cell). Each transport mechanism is likely to take up a range of ions. A basic problem is the interaction of ionic species during uptake of various heavy metal contaminants. After uptake by roots, translocation into shoots is desirable because the harvest of root biomass is generally not feasible. Little is known regarding the forms in which metal ions are transported from the roots to the shoots.

Plant uptake-translocation mechanisms are likely to be closely regulated. Plants generally do not accumulate trace elements beyond near-term metabolic needs. And these requirements are small ranging from 10 to 15 ppm of most trace elements suffice for most needs. The exceptions are “hyperaccumulator” plants, which can take up toxic metal ions at levels in the thousands of ppm. Another issue is the form in which toxic metal ions are stored in plants, particularly in hyperaccumulating plants, and how these plants avoid metal toxicity. Multiple mechanisms are involved. Storage in the vacuole appears to be a major one.

Water, evaporating from plant leaves, serves as a pump to absorb nutrients and other soil substances into plant roots. This process, termed evapotranspiration, is responsible for moving contamination into the plant shoots as well. Since contamination is translocated from roots to the shoots, which are harvested,

contamination is removed while leaving the original soil undisturbed. Some plants that are used in phytoextraction strategies are termed "hyperaccumulators." They are plants that achieve a shoot-to-root metal-concentration ratio greater than one. Nonaccumulating plants typically have a shoot-to-root ratio considerably less than one. Ideally, hyperaccumulators should thrive in toxic environments, require little maintenance and produce high biomass, although few plants perfectly fulfill these requirements.

Metal accumulating plant species can concentrate heavy metals like Cd, Zn, Co, Mn, Ni, and Pb up to 100 or 1000 times those taken up by nonaccumulator (excluder) plants. In most cases, microorganisms bacteria and fungi, living in the rhizosphere closely associated with plants, may contribute to mobilize metal ions, increasing the bioavailable fraction. Their role in eliminating organic contaminants is even more significant than that in case of inorganic compounds.

Conclusions

Plants have evolved highly specific and very efficient mechanisms to obtain essential micronutrients. Phytoremediation takes the advantage of the unique and selective uptake capabilities of plant root systems, together with the translocation, bioaccumulation, and contaminant degradation abilities of the entire plant body.

References

A. Gaur and A. Adholeya, "Prospects of arbuscular mycorrhizal fungi in phytoremediation of heavy metal contaminated soils," Current Science, vol. 86, no. 4, pp. 528–534, 2004.

R. Rakhshaee, M. Giahi, and A. Pourahmad, "Studying effect of cell wall's carboxyl-carboxylate ratio change of Lemna minor to remove heavy metals from aqueous solution," Journal of Hazardous Materials, vol. 163, no. 1, pp. 165–173, 2009.

R. R. Hinchman, M. C. Negri, and E. G. Gatliff, "Phytoremediation: using green plants to clean up contaminated soil, groundwater, and wastewater," Argonne National Laboratory Hinchman, Applied Natural Sciences, Inc, 1995, http://www.treemediation.com/Technical/Phytoremediation_1998.pdf.

I. Shtangeeva, J. V.-P. Laiho, H. Kahelin, and G. R. Gobran, "Phytoremediation of metal-contaminated soils. Symposia Papers Presented Before the Division of Environmental Chemistry," American Chemical Society, Anaheim, Calif, USA, 2004,

K. Cho-Ruk, J. Kurukote, P. Supprung, and S. Vetayasuporn, "Perennial plants in the phytoremediation of lead-contaminated soils," Biotechnology, vol. 5, no. 1, pp. 1–4, 2006.

M. M. Lasat, "Phytoextraction of metals from contaminated soil: a review of plant/soil/metal interaction and assessment of pertinent agronomic issues," Journal of Hazardous Substance Research, vol. 2, no. 5, pp. 1–25, 2000.

E. Pehlivan, A. M. Özkan, S. Dinç, and S. Parlayici, "Adsorption of Cu2+ and Pb2+ ion on dolomite powder," Journal of Hazardous Materials, vol. 167, no. 1–3, pp. 1044–1049, 2009.

S. Roy, S. Labelle, P. Mehta et al., "Phytoremediation of heavy metal and PAH-contaminated brownfield sites," Plant and Soil, vol. 272, no. 1-2, pp. 277–290, 2005.

D. Mohan and C. U. Pittman Jr., "Arsenic removal from water/wastewater using adsorbents—a critical review," Journal of Hazardous Materials, vol. 142, no. 1-2, pp. 1–53, 2007.

U.S. Department of Health and Human Services, Public Health Service Agency for Toxic Substances and Disease Registry. Division of Toxicology and Environmental Medicine. Arsenic. 2005,

H. Hasegawa, M. A. Rahman, T. Matsuda, T. Kitahara, T. Maki, and K. Ueda, "Effect of eutrophication on the distribution of arsenic species in eutrophic and mesotrophic lakes," Science of the Total Environment, vol. 407, no. 4, pp. 1418–1425, 2009.

WHO Regional Office for Europe, Air Quality Guidelines, chapter 6.1, Arsenic, Copenhagen, Denmark, 2nd edition, 2000.

P. Chutia, S. Kato, T. Kojima, and S. Satokawa, "Arsenic adsorption from aqueous solution on synthetic zeolites," Journal of Hazardous Materials, vol. 162, no. 1, pp. 440–447, 2009.

H. A. Andrianisa, A. Ito, A. Sasaki, J. Aizawa, and T. Umita, "Biotransformation of arsenic species by

activated sludge and removal of bio-oxidised arsenate from wastewater by coagulation with ferric chloride," Water Research, vol. 42, no. 19, pp. 4809–4817, 2008.
R. J. Ampiah-Bonney, J. F. Tyson, and G. R. Lanza, "Phytoextraction of arsenic from soil by Leersia oryzoides," International Journal of Phytoremediation, vol. 9, no. 1, pp. 31–40, 2007.
M. Vaclavikova, G. P. Gallios, S. Hredzak, and S. Jakabsky, "Removal of arsenic from water streams: an overview of available techniques," Clean Technologies and Environmental Policy, vol. 10, no. 1, pp. 89–95, 2008.
R. K. Sinha, S. Herat, and P. K. Tandon, "14 phytoremediation: role of plants in contaminated site management," in Book of Environmental Bioremediation Technologies, pp. 315–330, Springer, Berlin, Germany, 2004.
U. S. Department of Energy, "Plume Focus Area, December. Mechanisms of plant uptake, translocation, and storage of toxic elements. Summary Report of a workshop on phytoremediation research needs," 1994,
L. Erdei, G. Mezôsi, I. Mécs, I. Vass, F. Fôglein, and L. Bulik, "Phytoremediation as a program for decontamination of heavy-metal polluted environment," Acta Biologica Szegediensis, vol. 49, no. 1-2, pp. 75–76, 2005.

Synthesis of o- Alkeyl (Arayl) Trithiophasphates of Lanthanun:

Upendra Singh[1], Madhu Sharma[2], Jagat Pal Singh[3]
[1]Dept of Chemistry, RR College,Alwar (Rajasthan)
[2]Dept. of Chemistry, Govt. GD College for women,Alwar (Rajasthan)
[3]Govt College, Deeg (Rajasthan)
Email: dr usingh09@gmail.com

Abstract:
The complex of the type $La_2[S_3P(OR)]_3$where R = Me, Et, Pr^i, Bu^n amp Ph has been synthesized by reacting anhydrous Lanthanum (III) chloride with dipotasium salt of trithiophosphoric acids in refluxing methanol and finally extracted using benzene. The reaction is quite facile and are completed at room temperature mixing the reactants. These complexes have been characterized by elemental analysis molecular weight measurements, IR, UV(Electronic spectral) and multinuclear NMR (^1H and ^{31}P)Studies

Introduction:
The complexes of lanthanides and actinides have been the subject of many structural investigations during the last few years. These metals due to their large atomic size generally forms complexes with higher coordination numbers.
In recent years some workers have reported synthesis and structures of dithiophosphate derivatives of these metals however there appears to be no study on the respective O-alkyle(aryl) trithiophosphate derivatives of lanthanum therefore it was considered of interest to isolate lanthanum (III) O-alkyl (aryl) trithiophosphates and their adducts with heterocyclic tertiary amines. To study their pesticidal behaviour and some of their important reactions, it was thought to concentrate on O-alkyl(aryl) trithiophosphate derivatives of La. The continuing interest in this area is mainly due to the industrial utility of these compounds as well as their noval structural features.

Result and Recursion:
O-Alkyl (aryl) trithiohpophates of lanthanum have been synthesized by the reaction of anhydrous lanthanum chloride with the corresponding dipotasium salt of trithiophosphoric acids in refluxing methanol. The product were extracted using benzene.

$$2LaCl_3 + 3K_2[S_3P(OR)] \xrightarrow{\text{MeOH/Benzene}} La_2[S_3P(OR)]_3 + 6kcl$$

Where R = Me , Et , pri, Bu^n and ph

These complexes [table-1] are gray coloured solids, soluble in benzene, chloroform, methanol etc. and are insoluble in n-hexane, light petroleum. The complexes formed are non-volatile and tend to decompose by heating. Molecular weight measurements of freshly prepared complexes shows monomeric nature.
The complexes of the type $La2[S_3P(OR)]_3$ reacts with strong coordinating ligands as heterocyclic ditertiary amines to form addition complexes [table-2] in methanol, results in the increase of the coordination number of lanthanum from six to eight. A pink coloured compounds crystallize out by the reaction of respective lanthanum complex.

$$La_2[S_3P(OR)]_3 + N_2Cl_{10}H_8 \longrightarrow La_2[S_3P(OR)]_3.\ N_2C_{10}H_8$$

$$La_2[S_3P(OR)]_3 + N_2Cl_{12}H_8 \longrightarrow La_2[S_3P(OR)]_3.\ N_2C_{12}H_8$$

IR Spectra:
The IR spectra [table-3,4] show the following characteristic absorption bands
1. The absorption band found in the region 400-380 cm^{-1}us due to υ [La-S] mode vibration

indicating the complexation tendencies.

2. The absorption bands found in the regions 1095-990cm^{-1} and 1010-860 cm^{-1} have been assigned to **υ** [(P)- O – C] and **υ**[P-O-(C)] stretching vibration. In the adducts, the above absorption band are shifted towards higher frequencies than parent trithiophosphates.
3. A sharp intensity band observed in the region 700-650 cm^{-1} is due to **υ**[P = S] while it appears at 720-670 cm^{-1} in the adducts .
4. The absorption bands of medium intensity in the region 545-525 cm^{-1} could be ascribed to **υ**[P-S] vibrations and in adducts it observed in the region 605-560 cm^{-1}
   The shifting of the absorption towards higher wave-number indicating increase in the ionocity of the corresponding chemical linkage.

Electronic spectra:

The electronic spectra of lanthanum complexes and their adducts [table-5,6] have been recorded in the range 800-200nm is methanol. Generally two electronic transition bands have been observed in the ranges 234-224 nm and 268-264 nm for the complexes of the type La_2 [$S_3P(OR)]_3$while in the adducts, the broad absorption bands presence in the range 309-290 nm for $La_2[S_3P(OR)]_3$, $N_2C_{10}H_8$ and at 292-285 nm for $La_2(S_3P(OR)]_3$, $N_2C_{12}H_8$ type complexes

NMR Spectra [^{1}H and ^{31} P]

The ^{1}H NMR spectral data for their complexes and their adducts [table- 7-8] shows the characteristic resonance due to aromatic and alkoxyl protons. In adducts the spectra show resonance signals with minor up field shift for each type of trithiophosphates. A complex multiplet for aromatic protons has been observed for the adducts in the region 7.90-8.80 ppm and 8.20-9.35 ppm respectively. 31p NMR spectral data exhibit a down field shift of about 20.0 – 30.0 ppm with respect to values observed for the parent trithiophosphates.

Experimental

Dipotasium salts of o- alkyl (aryl) trithiophosphoric acids have been prepared by slow addition of trimethyl amine with respective alcohols to a solution of phosphorus pentasulfide in benzene.

The anhydrous lanthanum chloride was prepared by sintering $LaCl_3$, $7H_2O$ at 220-230^{0}C for 6-8 hrs in dried HCl gas.

Elemental analyses were carried out by standard procedures molecular weights were measured on a knauer-vapour pressure osmometer in benzene solution. IR spectra were recorded as KBr pellets of nujol mulls on a perkin-Elmer spectrophotometer modal 577 in the range 4000^{-1} -200 cm. H NMR in $CDCl_3$ and DMSO-d and 31p NMR in THF were recorded on a JEOL FX 900 spectrometer using TMS (for ^{1}H) and H_3PO_4 (for ^{31}P) as internal and external references respectively.

Synthesis of La_2 $[S_3P(OR)]_3$: An solution of anhydrous $LaCl_3$ was added to $K_2[S_3P(OR)]_3$ in refluxing methanol. To ensure the completion of Hu reaction the contents was refluxed for 6-8 hrs. And precipitate isolated by filtration. The product was dried under reduced pressure. The adducts of $La_2[S_3P(OR)]_3$ have been synthesized by a similar method and the relevant analytical data for the other complexes are listed in tables.

References:

1.B.Pkotavich, N.I Zemlyauskii I.V muraver and m.pvolosin Znobshchkhim 8317a (1959)
2. F. A cotton and G.wilkinson," Advanced inorjanic chemistry " vth edition elesvier (1988)
3. k.knistin B. utaG.EwaldG.k lays k ubich s Heneryk.Bernt and H. Gerald , z Naturforsch. Chem sci. B, 45,245, (1990)
4. U.s. pat no.2 , 820 , 049 , Ref Zhkhim, 83.179 (1959)
5. I.pchupp and p.eNewallis , J.org chem . 27,3832(1962)
6, O.N Grishina and L.mBezzubora , IZV. Akad.Nauk . USSR,
7. D Negoin , M . Negoin , But Inst. Politch, Bunuresh. SerKhin. 46-47, 146(1985)
8. AlokChaturvedi, Ph.DThesis , university of Rajasthan , Jaipur (1992)

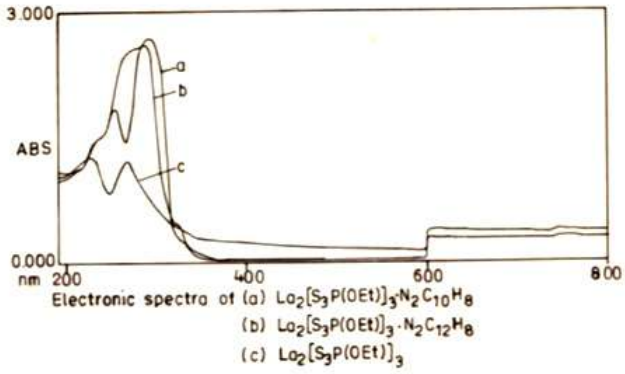

Table 1. – SOME PHYSICAL PROPERTIES OF THE COMPLEXES OF TYPE $La_2[S_3P(OR)]_3$

S.No	Compound	Physical State	Molecular Weight Found (calco.)
1	$La_2[S_3P(OMe)]_3$	Gray Solid (Powder)	733.99 (752.00)
2	$La_2[S_3P(OEt)]_3$	Gray Solid (Powder)	----------
3	$La_2[S_3P(OPr^i)_3$	Gray Solid (Powder)	803.20 (836.00)
4	$La_2[S_3P(OBu^n)]_3$	Gray Solid (Powder)	----------
5	$La_2[S_3P(OPh)]_3$	Gray Solid (Powder)	907.36 (938.00)

Table 2. – SOME PHYSICAL PROPERTIES OF THE COMPLEXES OF TYPE $La_2[S_3P(OR)]_3.N_2C_{10}H_8$ and $La_2[S_3P(OR)]_3.N_2C_{12}H_8$

S.No	compound	Physical satte	Molecular weight Found (caled.)
1	$La_2[S_3p(OMe)]_3.\ N_2C_{10}H_8$	Pink solid	888.21 (908.00)
2	$La_2[S_3p(OEt)]_3.N_2C_{10}H_8$	Pink solid	---------
3	$La_2[S_3p(OPr^i)]_3.N_2C_{10}H_8$	Pink solid	---------
4	$La_2[S_3p(OBu^n)]_3.\ N_2C_{10}H_8$	Pink solid	1002.26 (1034.000
5	$La_2[S_3p(OPh)]_3.\ N_2C_{10}H_8$	Pink solid	----------
6	$La_2[S_3p(OMe)]_3.N_2C_{12}H_8$	Pink solid	----------
7	$La_2[S_3p(OEt)]_3.N_2C_{12}H_8$	Pink solid	944.34 (974.00)
8	$La_2[S_3p(OPr^i)]_3.\ N_2C_{12}H_8$	Pink solid	987.28 (1016.00)
9	$La_2[S_3p(OBu^n)]_3.N_2C_{12}H_8$	Pink solid	---------
10	$La_2[S_3p(OPh)]_3.\ N_2C_{12}H_8$	Pink solid	1092.80 (1118.00)

Table 3. – SOME RELEVANT IR SPECTRAL DATA (IN Cm^{-1}) FOR THE COMPLEXES OF THE TYPE $La_2[S_3P(OR)]_3$

S.no	Compound	υ [(P)-O-c]	υ [P-O-(C)]	υ [P=S]	υ [P-S]	υ [La-S]
1	$La_2[S_3P(OMe)]_3$	1010 s	860 s	680 s	530 m	385 m
2	$La_2[S_3P(OEt)]_3$	1020 s	890 m	670 s	545 b	390 m
3	$La_2[S_3P(OPr^i)]_3$	1010 m	870 m	660 s	525 m	400 b
4	$La_2[S_3P(OBu^n)]_3$	990 m	870 s	650 s	540 b	390 b
5	$La_2[S_3P(OPh)]_3$	1095 s	1010 m	700 s	520 b	380 m

s = Sharp m= medium b= broad

Table 4. SOME RELEVANT IR SPECTRAL DATA (IN CM1) FOR THE COMPLESES OF THE TYPE

$La_2[S_3P(OR)]_3 . N_2C1_0H_8$ and $La_2[S_3P(OR)]_3 . N_2C1_2H_8$

S.no	Compound	υ [(P)-O-c]	υ [P-O-(C)]	υ [P=S]	υ [P-S]	υ [La-S]
1	$La_2[S_3p(OMe)]_3 . N_2C_{10}H_8$	1080 m	890 m	700 m	580 w	330 w
2	$La_2[S_3p(OEt)]_3 .N_2C_{10}H_8$	1130 m	930 m	685 m	605 b	340 m
3	$La_2[S_3p(OPr^i)]_3 . N_2C_{10}H_8$	1110 m	910 m	680 s	570 m	355 m
4	$La_2[S_3p(OBu^n)]_3 .N_2C_{10}H_8$	1090 s	920 m	680 s	600 m	330 w
5	$La_2[S_3p(OPh)]_3 .N_2C_{10}H_8$	1160 m	1030 b	720 m	590 w	320 w
6	$La_2[S_3p(OMe)]_3 .N_2C_{12}H_8$	1070 s	880 m	690 m	585 w	330 w
7	$La_2[S_3p(OEt)]_3 .N_2C_{12}H_8$	1120 s	910 b	680 s	590 m	330 w
8	$La_2[S_3p(OPr^t)]_3 .N_2C_{12}H_8$	1080 m	880 m	670 s	560 b	340 m
9	$La_2[S_3p(OBu^n)]_3 .N_2C_{12}H_8$	1080 s	895 m	680 m	580 m	330 w
10	$La_2[S_3p(OPh)]_3 .N_2C_{12}H_8$	1140 m	1020 m	710 m	570 b	355 m

s = Sharp m= medium b= broad w= weak

Table 5. -DATA FOR THE ELECTRONIC SPECTRAL STUDIES OF THE COMPLEXES OF THE TYPE $La_2[S_3P(OR)]_3$

s.no	Compound	Wave Length (In nm)
1	$La_2[S_3P(OMe)]_3$	266 227
2	$La_2[S_3P(OEt)]_3$	268 224
3	$La_2[S_3P(OPr^i)]_3$	264 226
4	$La_2[S_3P(OBu^n)]_3$	267 230
5	$La_2[S_3P(OPh)]_3$	267 234

Table 6. – DATA FOR THE ELECTRONIC SPECTRAL STUDIES OF THE COMPLEXES OF THE TYPE $La_2[S_3P(OR)]_3 .N_2C_{10}H_8$ and $La_2[S_3P(OR)]_3 .N_2C_{12}H_8$

s.no	Compound	Wave Length (In nm)
1	$La_2[S_3p(OMe)]_3 .N_2C_{10}H_8$	298
2	$La_2[S_3p(OEt)]_3.N_2C_{10}H_8$	289
3	$La_2[S_3p(OPr^i)]_3 .N_2C_{10}H_8$	302
4	$La_2[S_3p(OBu^n)]_3 .N_2C_{10}H_8$	309 290
5	$La_2[S_3p(OPh)]_3 .N_2C_{10}H_8$	294
6	$La_2[S_3p(OMe)]_3 .N_2C_{12}H_8$	292 274
7	$La_2[S_3p(OEt)]_{3.}$ $N_2C_{12}H_8$	288
8	$La_2[S_3p(OPr^t)]_3 . N_2C_{12}H_8$	285
9	$La_2[S_3p(OBu^n)]_{3.}$ $N_2C_{12}H_8$	289 272
10	$La_2[S_3p(OPh)]_{3.}$ $N_2C_{12}H_8$	283

s = Sharp m= medium b= broad w= weak

Table 7.- NMR SPECTRAL DATA FOR THE COMPLEXES OF THE TYPE $La_2[S_3P(OR)]_3$

S.no	Compound	^{1}H NMR Chemical Shifts in $CDCL_3$/DMSO-D_6 (In δ ppm)	^{31}P NMR Chemical shift in the (in δppm)
1	$La_2[S_3P(OMe)]_3$.	3.62 – 3.91 , m, (OMe)	102.63
2	$La_2[S_3P(OEt)]_3$.	1.38, t, 9H(Me) 3.54- 4.26, m, 6H(- OCH_2)	198.03
3	$La_2[S_3P(OPr^i)]_3$.	1.32- 1.40, d, 18H(Me) 4.53- 5.26, m 3H(OCH)	93.40
4	$La_2[S_3P(OBu^n)]_3$.	0.96, t, 9H (Me) 1.20 – 2.12, m 18H(CH_2) 3.63 – 4.33, m 6H(OCH_2)	94.74
5	$La_2[S_3P(OPh)]_3$	6.88, s, 15H(OPh)	98.64

S=singlet d=dublet t= triplet m= multiplet

Table 8.- – NMR SPECTRAL DATA FOR THE COMPLEXES OF THE TYPE $La_2[S_3P(OR)]_3N_2C1_0H_8$ and $La_2[S_3P(OR)]_3N_2C1_2H_8$

S.no	Compound	^{1}H NMR Chemical Shifts in $CDCL_3$/DMSO-d_6 (In δppm)	31p NMR Chemical shift in the (in δppn)
1	$La_2[S_3p(OMe)]_3 .N_2C_{10}H_8$	3.60 – 3.92, m (OMe) 7.90 – 8.60 m 8H($N_2C_{10}H_8$)	101.77
2	$La_2[S_3p(OEt)]_3 .N_2C_{10}H_8$	1.46, t, 9H(Me) 3.63 - 4.34, m 6H(-OCH_2) 8.00 – 8.80, m, 8H($N_2C_{10}H_8$)	97.88
3	$La_2[S_3p(OPr^i)]_3 .N_2C_{10}H_8$	1.38 - 1.46, d, 18H(me) 4.66 – 5.38, m, 3H(-OCH) 8.0 – 8.70, m, 8H($N_2C_{10}H_8$)	92.45
4	$La_2[S_3p(OBu^n)]_3 .N_2C_{10}H_8$	1.02, t, 9H(Me) 1.28 – 2.16, m, 12H(-CH_2) 3.76 – 4.44, m, 6H(-OCH_2) 8.0, m, 8H($N_2C_{10}H_8$)	94.35
5	$La_2[S_3p(OPh)]_3 .N_2C_{10}H_8$	7.18. s, 15H(OPh) 8.00 – 8.60,m, 8H($N_2C_{10}H_8$)	98.23
6	$La_2[S_3p(OMe)]_3 .N_2C_{12}H_8$	3.62 – 3.92, m (OMe) 8.20 – 9.20, b, 8H($N_2C_{12}H_8$)	99.67
7	$La_2[S_3p(OEt)]_3 .N_2C_{12}H_8$	1.47 ,t, 9H(Me) 3.62 – 4.32, m, 6H(-OCH_2) 8.30 – 9.35, b, 8H($N_2C_{12}H_8$)	97.29

8	$La_2[S_3p(OPr^t)]_3.$ $N_2C_{12}H_8$	1.36 – 1.48, d, 18H(Me) 4.68 – 5.34, m. 3H(-OCH) 8.20 – 9.30, b, 8 H($N_2C_{12}H_8$)	92.54
9	$La_2[S_3p(OBu^n)]_3.$ $N_2C_{12}H_8$	1.04, y, 9H(Me) 1.30 – 2.20, m, 12H(CH_2) 3.80 - 4.44, m, 6H(-OCH_2) 8.30 – 9.10, b, 8H($N_2C_{12}H_8$)	93.94
10	$La_2[S_3p(OPh)]_3.$ $N_2C_{12}H_8$	7.20 , s, 15H(OPh) 8.20 – 9.10,b, 8H($N_2C_{12}H_8$)	98.09

S=singlet d=dublet t= triplet m= multiplet

An Inventory Model For Deteriorating Items With Trade Credit And Advertisement Dependent Demand And Time Varying Holding Cost

[1]Anil Kumar Sharma and [2]Varsha Sharma

[12]Department of Mathematics, Raj Rishi Govt. Autonomous College, Alwar 301201 Rajasthan India

In the proposed research, we developed an economic order quantity inventory model for deteriorating items in which demand is deterministic function of selling price and advertisement cost. Time varying holding cost and trade credit under deteriorating environment is considered. In this model, shortages are allowed and fully backlogged. Here the supplier is allowed a credit limit to the customer during there is no interest charged applied but after the expiry of the certain time limit, the supplier will charge some interest. This model aids in minimizing the total inventory cost by finding the optimal cycle length, the optimal time length of replenishment and the optimal order quantity. The optimal solution of the model is illustrated with the help of numerical example. Also, the effect of changes in the different parameter on the optimal total cost is graphically presented.

KEYWORDS: Trade credit, Advertisement dependent demand, deterioration, time varying holding cost

1. Introduction

In the EOQ model, we assume that the supplier must be paid for the items as soon as the items are received, However, in practice, this may not be true. In today's business transactions, it is more and more to see that a supplier will allow a certain fixed period for setting the amount owed to him for the items supplied. The suppliers offer delay in payments to the retailers to buy more items and the retailers can sell the item before the closing of the delay time. As a result, the retailers sell the items and earn interests. Usually, there is no interest charge if the outstanding amount is paid within the permissible delay period. This provides opportunities to the retailers to accumulate revenue and earn interest by selling their items during the delay periods. This permissible delay in payments provides benefit to the supplier in as much as attracting new customers who consider it to be a type of price reduction and reduction in sells outstanding as some customers make payments on time in order to take advantage of permissible delay more frequently. In this direction, Goal [1985] extended the EOQ model under the conditions of permissible delay in payments. Liao, Tsai, and Su [2000] developed an inventory model for initial-stock-dependent consumption rate when a delay in payments is permissible. Alfares [2007] found out inventory model with stock dependent demand under variable holding cost. Shah, Soni, and Patel [2010] used an integrated approach for optimal unit price and credit period for deteriorating inventory system when the buyer's demand is price-sensitive. Recently Musa and Sani [2012] studied an inventory ordering policies of delayed deteriorating items under permissible delay in payments. Sarkar [2012c] framed an EOQ model with delay in payments and time- varying deterioration rate. Maihami and Abadi [2012] derived the joint control of inventory and its pricing for non-instantaneously deteriorating items under permissible delay in payments and partial backlogging.

Lin, Ouyang, and Dang [2012] developed a joint optimal ordering and delivery policy for an integrated supplier-retailer inventory model with trade credit and defective items. In the present competitive market, the selling price of an item is one of the important factors in selecting an item for use. It is commonly seen that higher selling price causes decrease in demand, whereas selling price has the reverse effect. Apart from price, the other marketing parameter which affects the demand is advertisement. Ii is commonly seen that a product is promoted through the advertisement in the wellknown print or electronic media or by other means to attract the customers. The purpose of this type of advertisement is to raise the demand of the product. hence it can be concluded that the demand of an item is a function of marketing cost and selling price of an item. Wang and Shang [2013] developed a

Supply chain channel strategy with quality and marketing effort-dependent demand. Bhunia &. Jaggi [2014] developed a two-warehouse inventory model for deteriorating items under permissible delay in payment with partial backlogging. Later on, Bhunia et. al [2015] proposed a two-storage inventory model for deteriorating items with variable demand and partial backlogging. Bhunia et. al [2016] developed a two-warehouse inventory model for deteriorating items under permissible delay in payment via particle swarm optimization. Bhunia et.al [2017] proposed a partially integrated production inventory model with interval valued inventory costs, variable demand and flexible reliability. Pal, B. [2018] developed an optimal production model with quality sensitive market demand, partial backlogging and permissible delay in payment. Sharma & Sharma [2018] proposed a deterministic inventory model with Weibull distribution deteriorating item with selling price and the time dependent demand rate.

In the present work, a deterministic inventory model for deteriorating items with instantaneous replenishment and permissible delay in payments is proposed in which the demand is a deterministic function of selling price and advertisement cost. In this model, deterioration rate and holding cost are linear and shortages are allowed and are fully backlogged. we have shown the suitable numerical examples to illustrate the model. sensitivity analysis of the optimal solution with respect to major parameters of the system is carried.

The rest of the paper is organized as follows: In Section 2, the notations and assumptions, which are used throughout this article, are described. In Section 3, the mathematical model to minimize the total annual inventory cost is established. Section

4 presents solution procedure to find the optimal length of time and order quantity. Numerical examples are provided in Section 6 to illustrate the theory and the solution procedure. This is followed by sensitivity analysis and conclusion.

2. Notations and Assumptions *2.1 Notations*

The following notations are used throughout this paper:

1. a is the scaling factor used in demand function which hold the condition $a > 0$.
2. s is the selling price per unit time.
3. b is the index of price elasticity used in demand function which hold the condition $b > 1$.
4. η is the shape parameter used in demand function which hold the condition $0 \leq \eta < 1$.
5. A_c is Advertisement cost per unit of item.
6. D is demand rate.
7. C_1 is the inventory shortage cost per unit time.
8. C_2 is the unit cost of an item.
9. A is the ordering cost of an order.
10. T is the fixed length of each ordering cycle.
11. q is the order quantity per cycle.
12. T_1 is the length of the period with positive stock of the item.
13. I_e is the interest earned per Rs./unit time.
14. I_p is the interest paid per Rs./ unit time.
15. M is the permissible delay in settling the account.
16. Q is the inventory level at time t.
17. TC is the total cost

2.2 Assumptions

To formulate the mathematical model, the following assumptions are made.

1. Replenishment is instantaneous.
2. Lead time is zero.
3. The permissible delay in payment is offered by the supplier to the retailer.
4. The demand rate is a deterministic function of selling price s and advertisement cost A_c per unit of item, i.e $D(A_c, s) = A_c^{\eta} a s^{-b}, a > 0, b > 1$, $0 \leq \eta < 1$ where a is the scaling factor, b is the index of price elasticity and η is the shape parameter.

5. The deterioration rate is time varying. $\theta(t) = \theta t$ is inventory deterioration rate.
6. Shortages are allowed and are fully backlogged.
7. The holding cost is linear with time dependent, $h(t) = (h + \alpha t)$, where α > 0, h > 0 is the inventory holding cost per unit time.
8. During time T_1, inventory is depleted due to deterioration and demand of the item. At time $T_1$the inventory becomes zero and shortages start occurring.

3. Formulation and the solution of the model

The inventory system is developed as follows: At time T_1 inventory level goes to zero and shortage occurs. During the period (0, T) can be described by differential equation (1) and (2) with boundary condition $Q(T_1) = 0$.

Based on the above description, the differential equation representing the inventory status are given by

$$\frac{dQ(t)}{dt} + \theta t.\, Q(t) = -D\ ;\ 0 \le t \le T_1 \qquad (1)$$

$$\frac{dQ(t)}{dt} = -D\ ; \qquad T_1 \le t \le T \qquad (2)$$

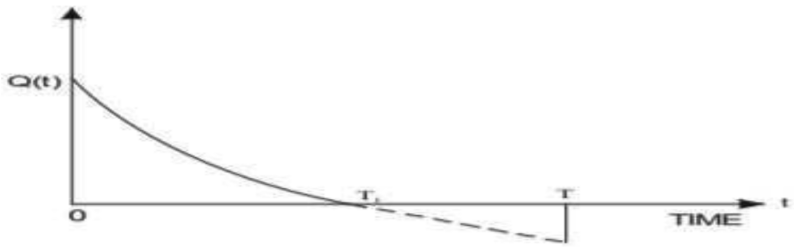

Figure 1. Graphical representation of the inventory system.

The solutions of the above differential equations (1) and (2) are given by

$$Q(t) = D[(T_1 - t) + \theta\left(\frac{T_3}{6} - \frac{T_3}{3} - \frac{T_{t2}}{2}\right) + \theta^2\left(\frac{T_2}{40} - \frac{T_5}{15} - \frac{T_{2T3}}{12} + \frac{T_{t4}}{8}\right)]$$

$$0 \le t \le T_1 \qquad (3) \text{ and}$$

$$Q(t) = -D(t - T_1) = D(T_1 - t)\ ; \qquad T_1 \le t \le T \qquad (4)$$

Now, we want to find the different inventory costs:

i. Annual ordering cost = A
ii. Interest charged = I_P
iii. Interest earned = I_E
iv. Stock loss due to deterioration $= \int_0^{T_1} e^{\theta t^2/2} dt - D\int_0^{T_1} dt$

$$= D\left[\frac{\theta T_3}{6} + \frac{\theta_2 T_5}{40}\right] \qquad (5)$$

v. Purchasing cost PC $= C_2\left[D\left(\frac{\theta T_{13}}{6} + \frac{\theta_2 T_{15}}{40}\right) + \int_0^T D\ dt\right]$ (6)

$$= C^2\ \frac{\theta T_{13}}{6}\ \frac{\theta_2 T_{15}}{40}\ D\,[+ \quad + T]$$

vi. Holding cost HC $= \int_0^{T_1}(h + \alpha t)Q(t)dt$

$$= Dh\,[\,1\ \frac{T_2}{2}\ \frac{\theta T_{13}}{12}\ \frac{\theta_2 T_{15}}{90}\ \frac{T}{6}\ \frac{\theta T_{14}}{40}\ \frac{\theta_2 T_{16}}{336}\ + \theta T_{14} + \theta_2 T_{16}] + \alpha D\,[T_{13} + \theta T_{15} + \theta_2 T_{17}] \qquad (7)$$

$$_1\int_{T_1}^{1} -D(t-T_1)dt = \frac{C_1D(T_2-T_1)^2}{}$$

(8) vii. Shortage cost SC= $-C^{T}$

The total cost of the system consists of the following elements:
Net stock loss due to deterioration, Net annual holding cost (HC), Annual Shortage cost (SC), Interest charged (I_P), Interest earned (I_E), Annual ordering cost (A) and purchasing cost (PC).

The following cases arise due to different types of delay periods:

Case (1): Payment at or before total depletion of inventory ($M \leq T_1$) i.e., the inventory not being sold after the due date and evaluate the interest payable IP_1 and interest earned IE_1 per cycle.

Case (2): Payment at or after depletion (M > T_1) i.e., the interest payable per cycle is zero because the supplier can be paid in full at time M, so only evaluate the interest earned which is earned during the positive inventory period plus the interest earned from the cash invested during time period (T_1, M) after the inventory is exhausted at time T_1.

Therefore, the total cost of the system per unit time is given by

$$\{TC_1, \quad M \leq T_1$$
$$TC_2, \quad M > T_1$$

Where TC_1 and TC_2 are discussed as follows.

Case 1: Payment at or before total depletion of inventory ($M \leq T_1$)

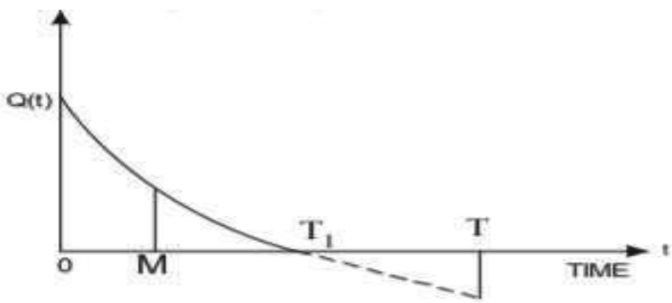

Figure 2. M < T_1

From the graph, the credit time expires on or before the inventory depleted completely to zero. The interest payable per cycle for the inventory not being sold after the due date M is interest payable in the time horizon when $M < t \leq T_1$

$$IP_1 = C_2 I_p \int_M^{T_1} Q(t)dt$$

$$= C_2 D I_p \left[\left(\frac{T_1^2}{2} + \frac{\theta T_1^4}{12} + \frac{\theta^2 T_1^6}{90}\right) - \left(MT_1 - \frac{M^2}{2}\right) - \theta\left(\frac{MT_1^3}{6} - \frac{M^4}{12} + \frac{M^3 T_1}{6}\right) - \theta^2\left(\frac{MT_1^2}{} - \frac{M^6}{} + \frac{M^3 T_1^3}{} + \frac{M^5 T_1}{}\right)\right] \quad (9)$$

$$40 \qquad 90 \qquad 36 \qquad 340$$

In addition, the interest earned per cycle IE_1 is the interest earned during the positive inventory level and is given by interest earned in the time horizon when $T_1 < t \leq 0$

$$IE_1 = \frac{C_2 D I_e T_{12}}{2} \tag{10}$$

The total cost per cycle per unit time = (ordering cost + shortage cost + inventory holding cost + purchase cost + interest charged - interest earned)/ T.

$$TC_1 = \frac{1}{2}\left[A + \frac{C_1 D (T - T_1)^2}{2} + \frac{T_{12}}{12} + \frac{\theta T_{14}}{90} + \frac{\theta_2 T_{16}}{} + Dh\left[\frac{T_{13}}{6} + \frac{\theta T_{15}}{40} + \frac{\theta_2 T_{17}}{336}\right] + C_2 D\left\{\frac{\theta T_{13}}{6} + \frac{\theta_2 T_{15}}{40} + + T\right\} + \alpha D\left[\frac{T_{12}}{2} + \frac{\theta T_{14}}{12} + \frac{\theta_2 T_{16}}{90}\right) - \left(MT_1 - \frac{M_2}{2}\right) - \theta\left(\frac{MT_{13}}{6} - \frac{M_4}{12} + \frac{M_3 T_1}{6}\right) - \theta_2\left(\frac{MT_1^2}{40} - \frac{M_6}{90} + \frac{M_3 T_{13}}{36} + \frac{M_5 T_1}{340}\right)\right\} - \frac{C_2 D I_e T_{12}}{2}\right] \tag{11}$$

Let $T_1 = \alpha T;\ 0 < \alpha < 1$

Here we have the total cost per cycle per unit time

$$TC_1 = \frac{1}{12}\left[A + \frac{C_1 D (1-\alpha)^2}{90} + Dh\left\{\frac{\alpha_2 T_2}{2} + \frac{\theta \alpha_4 T_4}{2} + \frac{\theta_2 \alpha_6 T_6}{2}\right\} T + \alpha D\left\{\frac{\alpha_3 T_3}{6} + \frac{\theta \alpha_5 T_5}{40} + \frac{\theta_2 \alpha_7 T_7}{336} + \right\} + C_2 D\left\{\frac{\theta \alpha_3 T_3}{6} + \frac{\theta_2 \alpha_5 T_5}{40} + + T\right\}\right.$$

$$\alpha_2 T_2 \qquad \theta \alpha_4 T_4 \qquad \theta_2 \alpha_6 T_6 \qquad M_2$$

$$+ C_2 D I_p \{ (\frac{}{2} \frac{}{12} \frac{}{90} \frac{}{2} + +) - (M\alpha T - \frac{}{})$$

$$- \theta \left(\frac{M\alpha_3 T_3}{6} - \frac{M_4}{12} + \frac{M_3 \alpha T}{6} \right)$$

$$- \theta_2 \left(\frac{M\alpha_5 T_5}{40} - \frac{M_6}{90} + \frac{M_3 \alpha_3 T_3}{36} + \frac{M_5 \alpha T}{340} \right) \}$$

$$- \frac{C_2 D I_e \alpha_2 T_2}{2}] \qquad (12)$$

Case 2: $M > T_1$ (Payment at or after depletion)

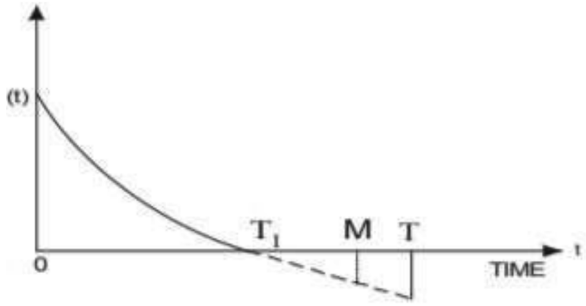

Figure 3. M > T_1

In this case, the interest payable per cycle is zero, i.e., $IP_2 = 0$, when $T_1 < M \leq T$ because the supplier can be paid in full at time M, the permissible delay. Thus, the interest earned per cycle is the interest earned during the positive inventory period plus the interest earned from the cash invested during time period (T_1, M) after the inventory is exhausted at time T_1, and is given by

$$IP_2 = 0 \qquad (13)$$

$$IE_2 = C_2 I_e \int_0^{T_1} D.t\, dt + C_2 I_e (M - T_1) \int_0^{T_1} D dt \qquad (14)$$

$$= \left(M - \frac{1}{2} \right) C_2 I_e D T_1^{T} \qquad (15)$$

The total cost per cycle per unit time = (ordering cost + shortage cost + inventory holding cost + purchase cost + interest charged - interest earned)/ T.

$$TC_1 = \frac{1}{2} [A + \frac{}{2} \frac{}{12} + Dh \{ \frac{C_1 D (T - T_1)_2}{90} + \frac{}{} + \frac{T_{12}}{} \} T \quad \theta T_{14} \quad \theta_2 T_{16}$$

$$+ \alpha D \left\{ \frac{T_{13}}{6} + \frac{\theta T_{15}}{40} + \frac{\theta_2 T_{17}}{336} \right\} - C_2 I_e D T_1 \left(M - \frac{T_1}{2}\right)] \qquad (16)$$

Let $T_1 = \alpha T; 0 < \alpha < 1$

Here we have the total cost per cycle per unit time

$$TC_2 = \frac{1}{12}\left[A + \frac{C_1 D(1-\alpha)^2}{90} + Dh \left\{ \frac{\alpha_2 T_2}{2} + \frac{\theta \alpha_4 T_4}{2} + \frac{\theta_2 \alpha_6 T_6}{2} \right\} T \right.$$

$$+ \alpha D \left\{ \frac{\alpha_3 T_3}{6} + \frac{\theta \alpha_5 T_5}{40} + \frac{\theta_2 \alpha_7 T_7}{336} \right\}$$

$$\left. - C_2 I_e D T \left(M - \frac{\alpha T}{2}\right)\right] \qquad (17)$$

4. Solution Procedure

Our aim is to minimize the total inventory cost by finding the optimal cycle length. In order to find the optimal solution T^* and to minimize the annual total relevant cost, we take the first and second derivatives of TC_i with respect to T. The necessary and sufficient condition for minimization of TC_i(T) respectably $\frac{d}{dT} TC_i(T) = 0$

and $\frac{d^2}{dT^2} TC_i(T) > 0$ Where $i = \{1, 2\}$

$$\frac{dTC_1(T)}{dT} = \frac{-A}{T} + \frac{C_1 D(1-\alpha)^2}{12} = \left[\frac{\alpha^2}{2} + \frac{\theta \alpha^4 T^2}{2} + Dh \left\{ \frac{\theta^2 \alpha^6 T^4}{2 + 4} + \frac{\theta \alpha^3 T}{18} \right\} \right.$$

$$+ \alpha D \left\{ \frac{\alpha_3 T}{3} + \frac{\theta \alpha_5 T_3}{10} + \frac{\theta_2 \alpha_7 T_5}{56} \right\} + C_2 D \left\{ \frac{\theta \alpha_3 T}{3} + \frac{\theta_2 \alpha_5 T_3}{10} \right\}$$

$$+ C_2 D I_p \left\{ \left(\frac{\alpha_2}{2} + \frac{\theta \alpha_4 T_2}{4} + \frac{\theta_2 \alpha_6 T_4}{18} \right) - \frac{M^2}{(2T_2)} - \theta \left(\frac{M \alpha_3 T}{3 + 12T_2} - \frac{M^4}{10} + 90T_2 - \frac{M \alpha^2 T^3}{18} \right) - \theta^2 \left(\frac{M^6}{\ } - \frac{M^3 \alpha^3 T}{\ } \right) \right\} - C_2 D I_e \alpha^2 \Big] = 0 \qquad (18)$$

$$\frac{d^2TC_1(\mathrm{T})}{dT} = \frac{2A}{T^3} + Dh\left\{\frac{\theta\alpha^2T}{10} + \frac{2\theta^2\alpha^6T^3}{56}\right\} + \alpha D\left\{\frac{\alpha^3}{2} + \frac{3\theta\alpha^5T^2}{9} + \frac{5\theta^2\alpha^7T^4}{56}\right\}$$

$$+ C_2D\left\{\frac{\theta\alpha^3}{2} + \frac{3\theta^2\alpha^5T^2}{9}\right\} + C_2DI_p\left\{\left(\frac{\theta\alpha^4T}{10} + \frac{2\theta^2\alpha^6T^3}{56}\right)\right\} + (T_3)$$

$$+ \theta\left(-M\overline{3\alpha^3} + 6\overline{MT}^4{}_3\right)^2\left(-\frac{3M10\alpha^2T^2}{45MT^6{}_3} + \frac{M18^3\alpha^3}{}\right) \qquad (19)$$

$$) + \theta$$

By solving the equation (18), we get the optimal value of T^*. Moreover, T satisfies the equations $\frac{d^2TCdT12(\mathrm{T})}{} > 0$.

Now

$$\overline{dTCdT^2}(T) = \left[-\mathrm{TA}_2 + C^4D(12-\alpha)^2 + Dh\left\{\alpha2^2 + \theta\alpha4^4T^2 + \theta^2\alpha18^6T^4\right\} + \alpha D\left\{\alpha3^3T + \theta\alpha10^5T^3 + \frac{\theta2\alpha7T5}{56}\right\} - C_2DI_eT(M-\alpha T)\right] = 0 \qquad (20)$$

and

$$\frac{d^2TC_2(\mathrm{T})}{dT} = \frac{2A}{T^3} + Dh\left\{\frac{\theta\alpha^4T}{10} + \frac{2\theta^2\alpha^6T^3}{56}\right\} + \alpha D\left\{\frac{\alpha^3}{2} + \frac{3\theta\alpha^5T^2}{9} + \frac{5\theta^2\alpha^7T^4}{56}\right\}$$

$$+ C_2DI_e(-M + 2\alpha T) \qquad (21)$$

By solving the equation (18), we get the optimal value of T_*. Moreover, T satisfies the equations $\frac{d^2TC22(\mathrm{T})}{dT} > 0$

5. Numerical Example

Consider an inventory system with the following data:

Let $A_c = 3000, a = 40{,}000, \eta = 0.4, s = 900, b = 2.59, A = 6000, M = 0.055, h =$

$0.4, C_1 = 1.2, C_2 = 20, \alpha = 0.1, \theta = 0.01, I_P = 0.15, I_E = 0.12$ in appropriate units.

Then we obtain the optimal solution as follows:

Case 1:

$\{t_1{}^* = 1.012,\ T^* = 1.88,\ Q^* = 341.3527,\ TC_1{}^* = 18776.078\}$

Case 2:

$\{t_1{}^* = 0.9572,\ T^* = 1.5430,\ \quad Q^* = 275.3527,\ TC_2{}^* = 17950.674\}$

Among the above solutions, the better solution is $\{t_1{}^* = 0.9572,\ T^* = 1.5430, Q^* = 275.3527,\ TC_2{}^* = 17950.674\}$.

Figure 4 shows that the total cost decreases with T and TC attains the minimum value 17950.674 at T= 1.5430. If T crosses 1.5430, the total cost then increases. From Figure 4, it is observed that the total cost is a convex function with respect to T.

Similarly Figure 5 shows that the convexity of the total cost function.

6. **Sensitivity Analysis**

We now study the effects of changes in the value of the system parameters $A_c, a, \eta, b, A, h, C_1, C_2, \alpha, \theta$ on the optimal replenishment policy of the example. We change one parameter at a time keeping the other parameters unchanged. The results are summarized in table 1.

Based on the numerical results, we obtain the following managerial phenomena:

1. When the advertisement cost Ac is increasing, the cycle length, the order quantity, and the total cost are highly increasing. That is the minimum advertisement cost will minimize the total cost of the retailer.
2. When the parameter a is increasing, the cycle length, the order quantity, and the total cost are also increasing.
3. When the parameter b is increasing, the cycle length, the order quantity, and the total cost are highly decreasing.
4. When the parameter η is increasing, the cycle length and the order quantity are increasing and the total cost changes variably.
5. When the holding cost h is increasing, the cycle length and the order quantity are decreasing and the total cost is increasing. That is, the minimum cost for holding the items will minimize the total cost of the retailer.
6. When the deterioration rate θ is increasing, the optimal cost is decreasing and the order quantity is increasing.

Table 1. Sensitivity analysis for various inventory parameters.

Parameter	Parameter value	t_1	T	Q	TC
A_c	1500	0.709	1.8481	133.27	17950.674
	3000	1.143	1.9557	162.61	18776.0230
	4500	1.354	1.9907	212.39	21728.7074
a	20,000	0.4225	1.3001	144.35	8773.3654
	40,000	1.1412	1.3657	162.61	8788.0230
	60,000	2.3700	1.4222	186.24	8849.1868
b	2.4	1.1692	1.3693	164.29	8928.9701
	2.59	1.2140	1.1657	162.61	8788.0230
	2.8	1.1412	1.0619	160.88	8643.5586
η	0.2	1.0786	1.6346	132.22	9601.4801
	0.4	1.1412	1.3654	162.61	8788.0230
	0.6	1.0948	1.2604	213.21	8194.0680
h	0.4	1.1412	1.6314	341.55	1738.1270
	0.8	1.1438	1.1412	340.36	1779.6013
	1.2	1.1126	1.0794	338.58	1821.0703
θ	0.01	1.2140	1.1412	342.44	1830.9046
	0.05	1.1412	1.0654	346.14	1779.6013
	0.09	1.0794	1.789	349.36	2845.2377

7. Conclusion

In this paper, an economic order quantity inventory model for deteriorating items in which demand is deterministic function of selling price and advertisement cost is developed where delay in payment is allowed. In this model, deterioration rate and holding cost are linear and shortages are allowed and are fully backlogged. Supplier offers credit period to the retailer who has the reserve money to make the payments, but decides to avail the benefits of credit limit. Furthermore, numerical example and sensitivity analysis was

carried out with respect to the key parameters and useful managerial insights were obtained. Graphical illustration is also given to analyze the efficiency of the model clearly.

The proposed models described some realistic features that are likely to be associated with some kinds of inventory. The model is very useful in retail businesses such as that of electronic components, fashionable clothes, domestic goods and other products.

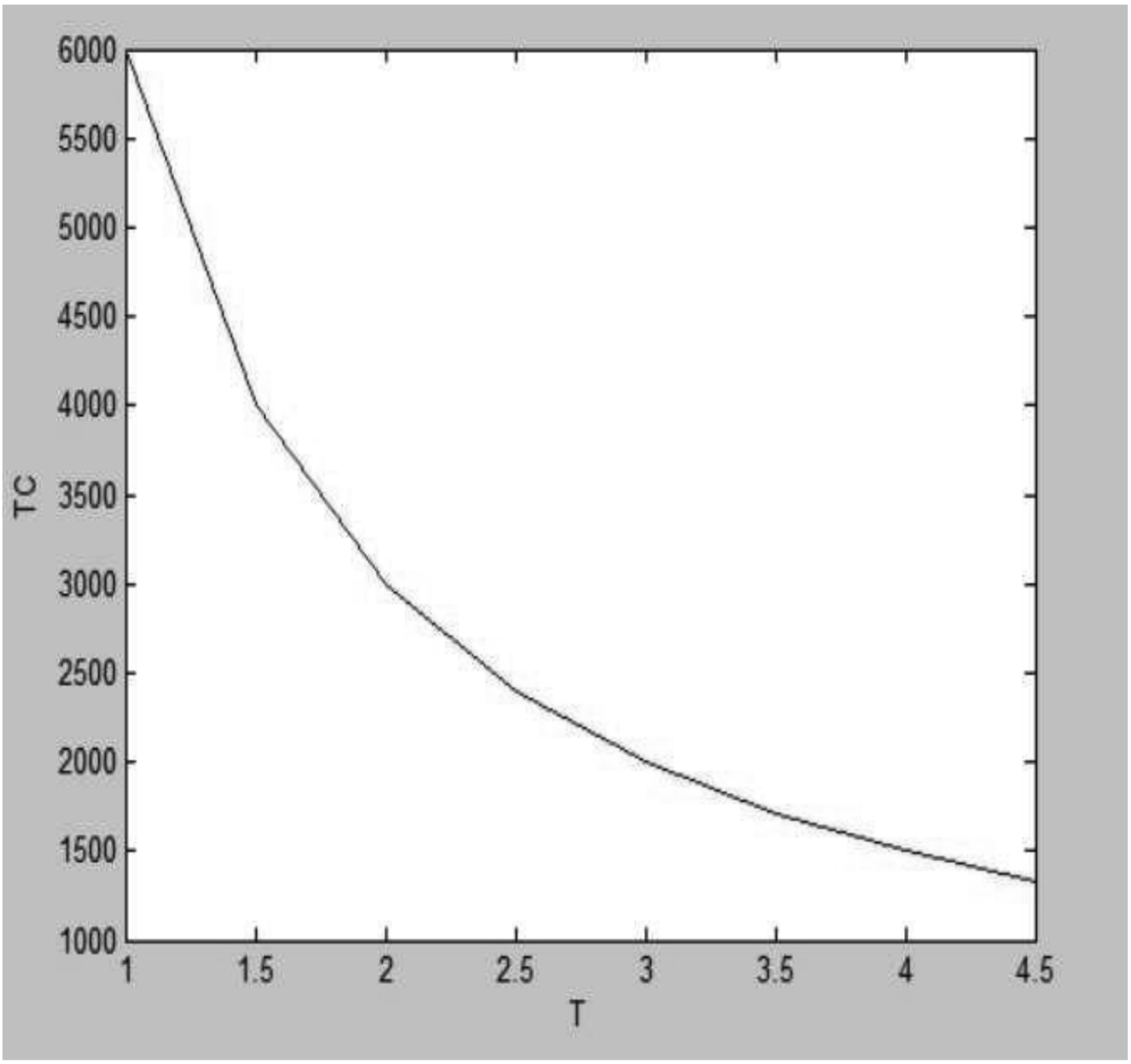

Figure 4. The total cost with respect to T for case 1.

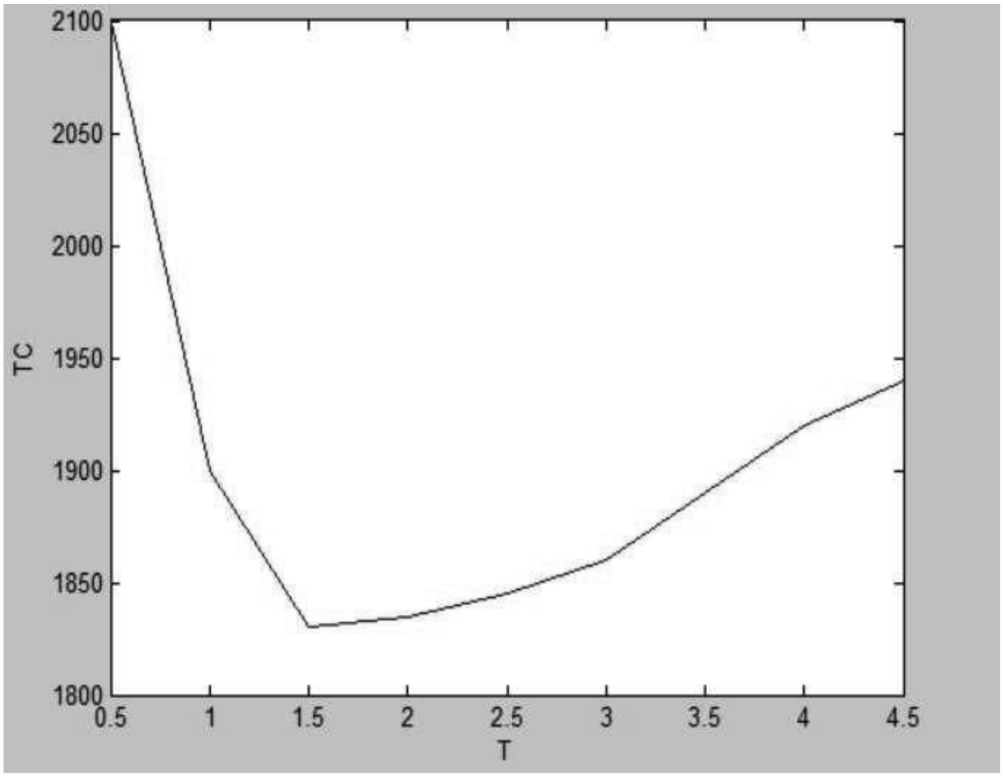

Figure 5. The total cost with respect to T for case 2

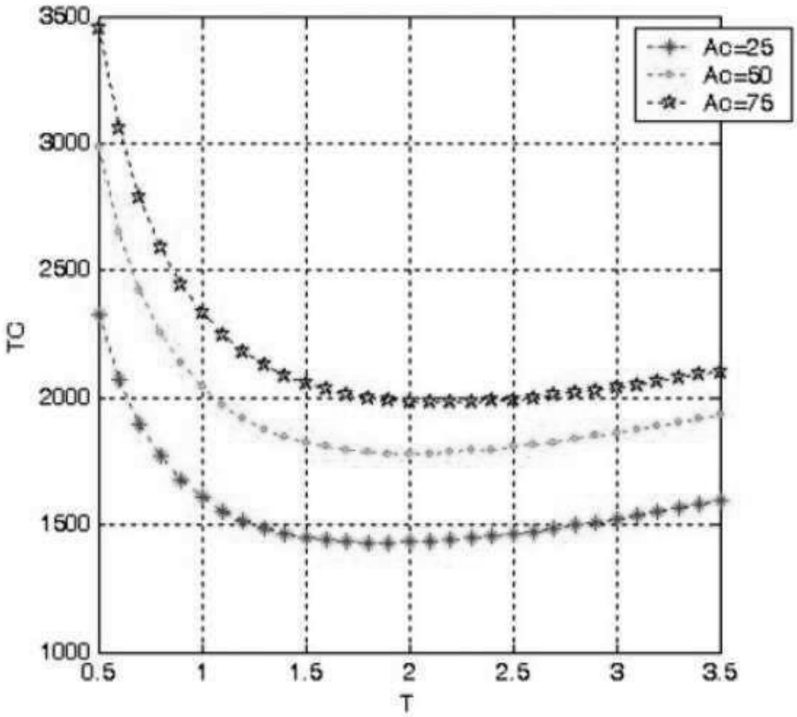

Figure 14. Total cost vs. cycle length for different values of A_c

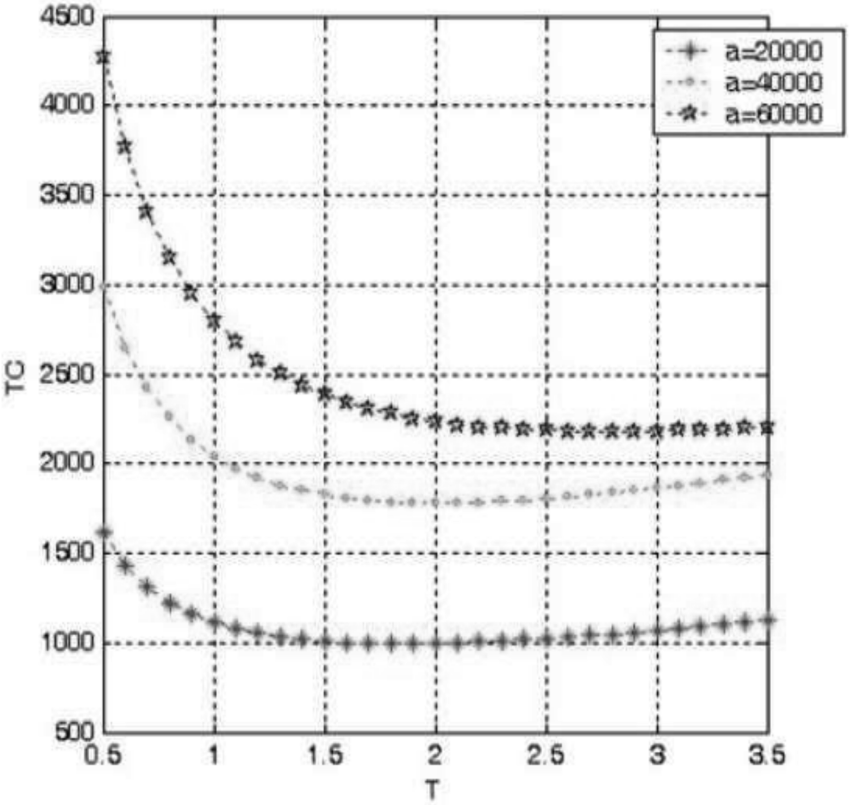
a=20000
a=40000
a=60000
TC
T
4500
4000
3500
3000
2500
2000
1500
1000
500
0.5
1
1.5
2
2.5
3
3.5

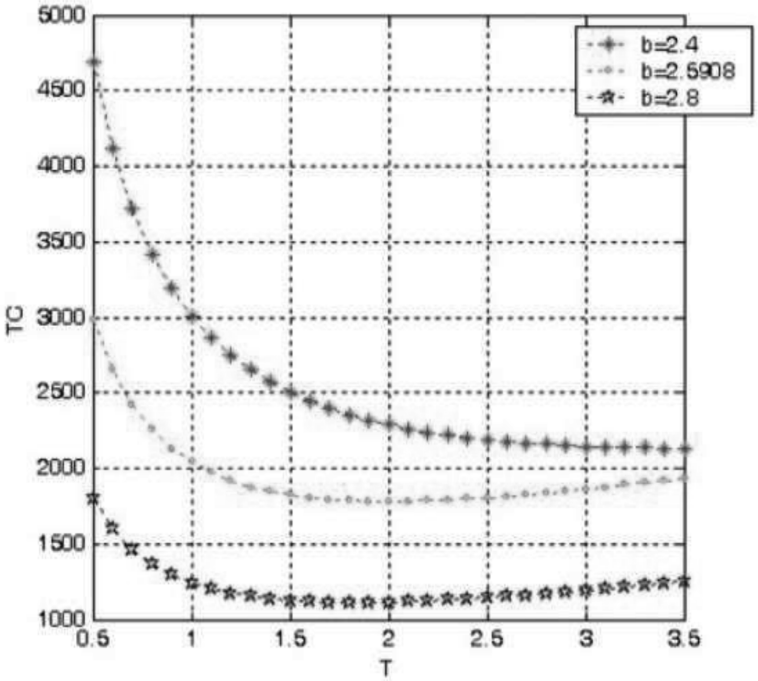
b=2.4
b=2.5908
b=2.8
TC
T
5000
4500
4000
3500
3000
2500
2000
1500
1000
0.5
1
1.5
2
2.5
3
3.5

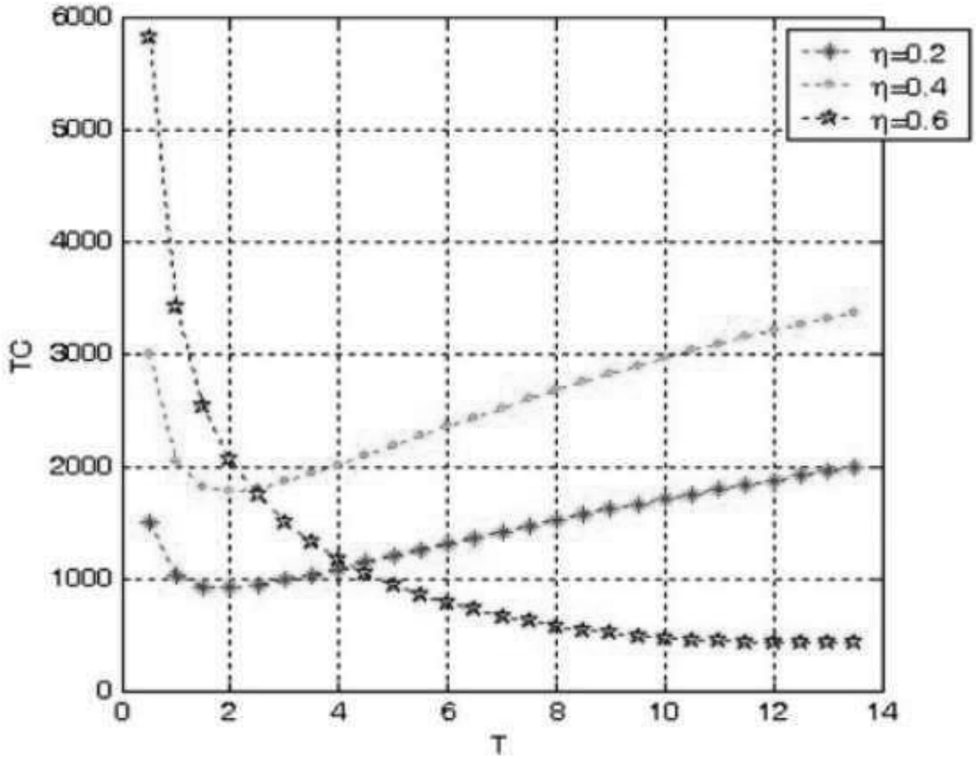
6000
5000
4000
3000
2000
1000
0
TC
0
2
4
6
8
10
12
14
T
η=0.2
η=0.4
η=0.6

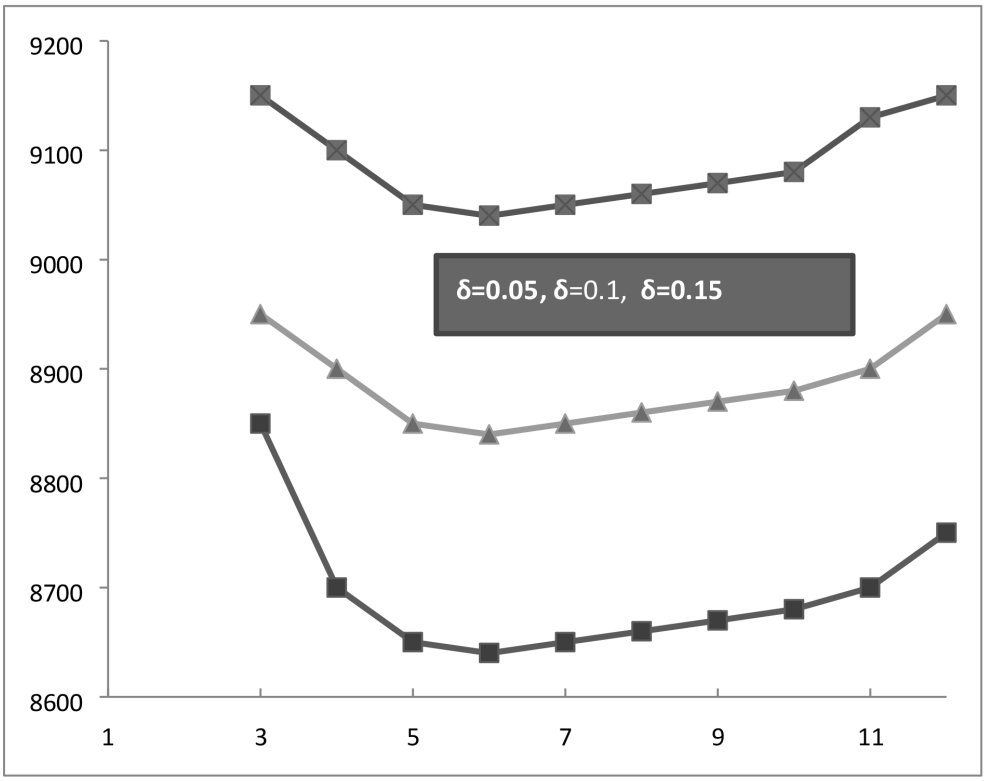
9200
9100
9000
8900
8800
8700
8600
1
3
5
7
9
11
δ=0.05, δ=0.1, δ=0.15

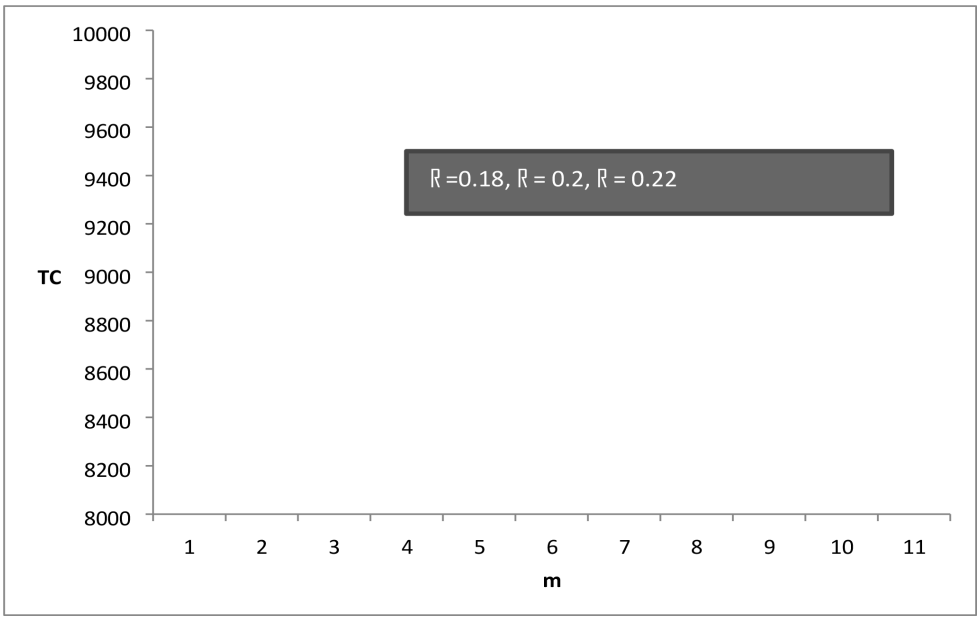

References

1. A.K. Bhunia, A.A. Shaikh and L. Sahoo. (2016). A two-warehouse inventory model for deteriorating items under permissible delay in payment via particle swarm optimization. *Inter. J. Logistics Syst. Manag. 24 (2016) 45–69.*
2. A.K. Bhunia, A.A. Shaikh, G. Sharma and S. Pareek. (2015). A two-storage inventory model for deteriorating items with variable demand and partial backlogging. J. Industrial Prod. Eng. 32, 263–272.
3. A.K. Bhunia, A.A. Shaikh, L.E. Cardenas−B´arr'. (2017). A partially integrated production inventory model with interval valued inventory costs, variable demand and flexible reliability. *Appl. Soft Comput. 55 (2017) 491– 502.*
4. A.K. Bhunia, C.K. Jaggi, A. Sharma and R. Sharma. (2014). A twowarehouse inventory model for deteriorating items under permissible delay in payment with partial backlogging. *Appl. Math. Comput. 232, 1125–1137.*
5. Alfares, H. K. (2007). Inventory model with stock-level dependent demand rate and variable holding cost. *International Journal of Production Economics, 108, 259–265.*
6. Goyal, S. K. (1985). Economic order quantity under conditions of permissible delay in payments. *Journal of the Operational Research Society, 36, 335– 338.*
7. Liao, H. C., Tsai, C. H., & Su, C. T. (2000). An inventory model with deteriorating items under inflation when a delay in payment is permissible. *International Journal of Production Economics, 63, 207–214.*
8. Lin, Y. J., Ouyang, L. Y., & Dang, Y. F. (2012). A joint optimal ordering and delivery policy for an integrated supplier – Retailer inventory model with trade credit and defective items. *Applied Mathematics and Computation, 218, 7498–7514.*
9. Maihami, R., & Abadi, I. N. K. (2012). Joint control of inventory and its pricing for non-instantaneously deteriorating items under permissible delay in payments and partial backlogging. *Mathematical and Computer Modeling, 55, 1722–1733.*
10. Musa, A., & Sani, B. (2012). Inventory ordering policies of delayed deteriorating items under permissible delay in payments. *International Journal of Production Economics, 136, 75–83.*
11. P. Ma, Wang, H. and Shang, J. (2013). Supply chain channel strategies with quality and marketing effort-dependent demand. *Inter. J. Prod. Econ. 144, 572–581.*
12. Pal, B. (2018). Optimal production model with quality sensitive market demand, partial

backlogging and permissible delay in payments. *Rairo-Oper. Res. 52 (2018) 499–512.*

13. Sarkar, B. (2012c). An EOQ model with delay in payments and time varying deterioration rate. *Mathematical and Computer Modeling, 55, 367–377*
14. Shah, N. H., Gor, A. S., & Wee, H. M. (2010). An integrated approach for optimal unit price and credit period for deteriorating inventory system when the buyer's demand is price sensitive. *American Journal of Mathematical and Management Sciences, 30, 317–330.*
15. Sharma & Sharma. (2018). A deterministic inventory model with Weibull distribution deteriorating item with selling price and the time dependent demand rate. *International academy of physical Sciences, Vol.21 No.1: 31-38.*

Spectrophotometric Determination of Vanadium (V) with Schiff base derived from Pyridine -2- Carboxaldehyde and 2- Amino Pyridine by preliminary adsorption on Polyurethane foam

Dr. Sunita Tandon
Department of Chemistry
Raj Rishi College, Alwar, Rajasthan

Abstract

The Spectrophotometric determination of Vanadium (V) by adsorption of its pyridine-2-carbaldehyde-2 Amino pyridine complex after adsorption on polyurethane foam is described. The complex is eluted from the foam with chloroform and absorbance is measured at 400nm. Beer's law is obeyed in the concentration range 5-90 microgram of vanadium. The molar absorptivity was found to be $2.3108*10^4$ $lmol^{-1}cm^{-1}$ and sensitivity being $1.14*10^{-2}$ microgram cm^{-2} for the absorbance of 0.001.

The effect of various parameters namely PH, reagent, adsorbent, shaking time and diverse ions have also been investigated.

Introduction:

Vanadium plays a vital role in enzyme reactions and nitrogen fixation.[1] It stimulates growth of plants and animals[2,3] and it is an essential micronutrient in many organisms responsible for health and disease.[4]. Presently, for determination of vanadium in bio- samples, 8 hydroxyquinoline[5] is used. The defects of this method are lack of selectivity and the narrow PH range.

Hulcher (1960) employed benzohydroxamic acid but there is also interference with iron (III).[6] Since 1960 N- phenyl –Benzohydroxamic acid has been widely used as a versatile reagent for colourmetric determination of vanadium, especially because of high selectivity and freedom from interference of iron (III).[7]

Among the other few reagents proposed for the identification of vanadium[8] mention may be made of hydrogen perioxide, -benzoinoxime and diaminobenzidine. Recently, p aminophenyl mercapto acetic acid has been used as a new diazotisable amine for the spectrophotometric determination of nitrite cercium and chromium based on azo dye formation. Chug and M. Kumar recently derived a new Schiff base[9] from 2 –furfural –dehyde and p-aminophenyl mercaptoacetic acid for use as a reagent for the identification of Vanadium (V).

Rana et al[10] synthesized and characterized complexes of V) (Ii) with tetradentate SB derived from ethylene diamine and 4-benzoyl-1-phenyl-3-methyl 2-prazdine-5-one. A newly synthesized Schiff base from pyridine -2-carboxaldehyde and 2 amino pyridine poses interesting analytical applications. "Solid –liquid extraction" technique using polyurethane foam has been used for extracting Vanadium (V). the synthesized Schiff vase is more selective reagent for the determination of Vanadium (V) out of different reagents employed for the photometric determination [11-15] of vanadium (V)

Procedure:

An aliquot (1.0 ml)of standard Vanadium (V) solution containing 15-90microgram of Vanadium was taken in a beaker and to it was added 2.5ml of 0.2% Schiff base solution. The pH was adjusted tom3.0. The volume was made to 10ml by adding water. The contents were allowed to stand for 2 minutes for complete development of color. Now to it seven already prepared polyurethane foam pieces were added. The flask was stoppered and shaken for 60secs to allow the metal complex formed to be adsorbed on the foam. The foam pieces containing the adsorbed complex were manually squeezed with the glass plunger. These foam pieces containing the adsorbed vanadium complex were transferred to glass beaker. The complex was eluted from the foam by squeezing with the two portions of 2.5ml chloroform. 2.0gm of anhydrous sodium sulphate was added to remove traces of water. Absorbance was measured in 1 cm cell in the region

3.70-560nm wavelength. Calibration curve was constructed at the similar conditions.

Results and discussion

Absorption Spectra:

A sample solution containing of 60microgm of vanadium (V)2.5ml of 0.2%reagent (SB_1) solution and 2.0ml of buffer solution was added to adjust the Ph3.0. all these contents were treated according to the recommended procedures All absorbance measurements were carried out at 400nm wavelength.

Fig 3.0 B shows the absorption spectra of vanadium (V) complex. The maximum absorption is observed at 400nm.

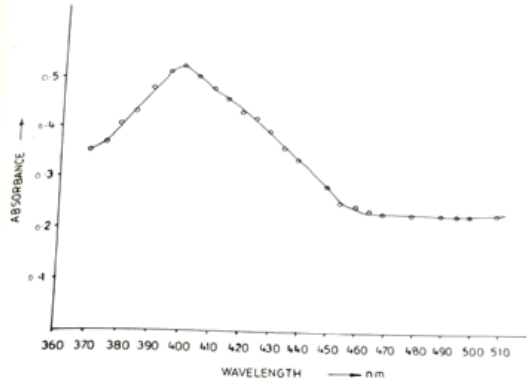

FIG - 3·0(B) ABSORPTION SPECTRA OF VANADIUM

VANADIUM(V)	:	60 µg
pH	:	3.0
0.2% REAGENT SOLUTION	:	2.5 ml
POLYURETHANE FOAM	:	7 PIECES
SHAKING TIME	:	120 Sec.

Effect of PH

The maximum and almos 'H range 2.0-6.0. therefore pH of the solution was taken to be 3.0 for all absorbance measurements.

Results are shown in following figure and table

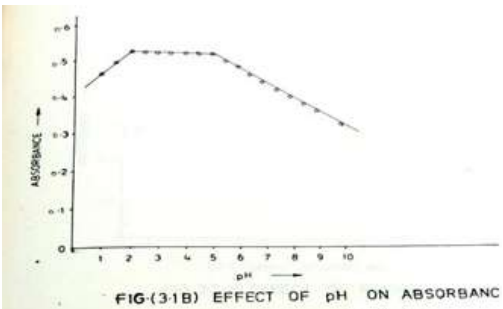

FIG-(3·1B) EFFECT OF pH ON ABSORBANC

VANADIUM (V)	:	60 µg
WAVELENGTH	:	400 nm
0.2% REAGENT SOLUTION	:	2.5 ml
POLYURETHANE FOAM	:	7 PIECES
SHAKING TIME	:	120 Sec

Table 3.1 (B) : Effect of pH.

pH	Absorbance at 400 nm
1.0	0.458
1.5	0.488
1.8	0.502
2.0	0.523
2.5	0.523
3.0	0.524
3.5	0.524
4.0	0.520
4.5	0.523
5.0	0.522
5.5	0.500
6.0	0.488
6.5	0.467
7.0	0.454
7.5	0.432
8.0	0.410
8.5	0.389
9.0	0.365
10.0	0.342

V (V) : 60 µg;
0.2% Reagent : 2.5 ml;
Shaking Time : 120 sec.;
Polyurethane Foam : 7 Pieces.

Effect of reagent Solution

In order to investigate the effect of the reagent concentration on the absorbance of vanadium (V) complex solution, different amounts of the reagent solution were added to the solution containing 60microgram of Vanadium (V) at Ph 3.0. The addition of 1.5 to 6.0ml of the reagent solution gave the maximum and almost same absorbance. Hence, 2.5ml of the reagent solution was considered the suitable quantity to be used for all absorbance measurements. The results are shown in following table and figure

Table 3.2 (B) : Effect of Reagent Concentration.

0.2% Reagent	Absorbance at 400 nm
0.5	0.487
1.0	0.499
1.5	0.524
1.8	0.522
2.0	0.524
2.5	0.523
3.0	0.524
3.5	0.523
4.0	0.525
4.5	0.524
5.0	0.525
5.5	0.520
6.0	0.510
6.5	0.515
7.0	0.485
7.5	0.475
8.0	0.475
9.0	0.475
10.0	0.450

V (V) : 60 µg;
pH - 3.0
Polyurethane Foam : 7 Pieces;
Shaking Time : 120 Sec.

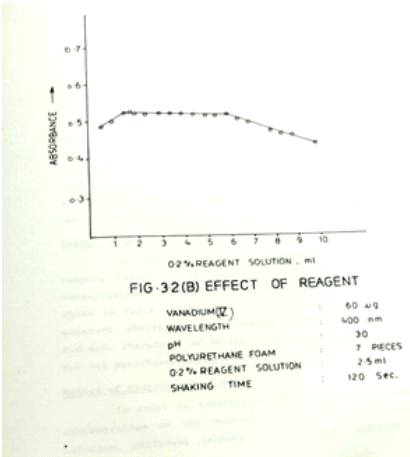

Effect of adsorbent

The effect of adsorbent on the adsorbance measurements was determined by adding different number of prepared polyurethane foam pieces, in the vanadium (V) complex solution. The absorbance increased with the addition of 1-3 polyurethane pieces then achieves maximum and almost constant value upto 9.0. Therefore seven foam pieces were taken for all absorbance measurements. The results are shown in figure and table

Table 3.3 (B) : Effect of Adsorbent.

No. of Polyurethane Foam Pieces used	Absorbance 400 nm
1	0.480
2	0.490
3	0.500
4	0.498
5	0.500
6	0.514
7	0.500
8	0.524
9	0.499
10	0.490

V (V) : 60 µg
pH : 3.0
0.2% Reagent : 2.5 ml;
Shaking Time : 120 Sec.

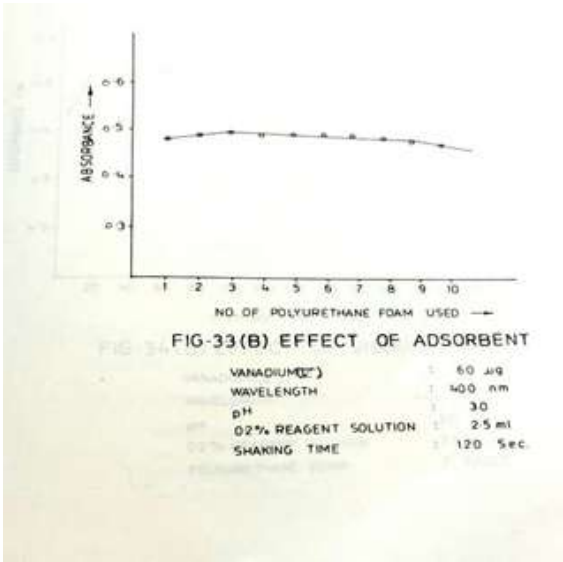

Effect of shaking time

Vanadium solution was allowed to stand in contact with Schiff base solution for two minutes. Then the complex was shaken for varying period of time i.e. from 5-300 seconds. Absorbance first increases, attains maximum and constant value from 20 sec to 160 seconds as shown in figure. So shaking time of

120 sec was chosen for all absorbance measurements
The results are shown in figure and table

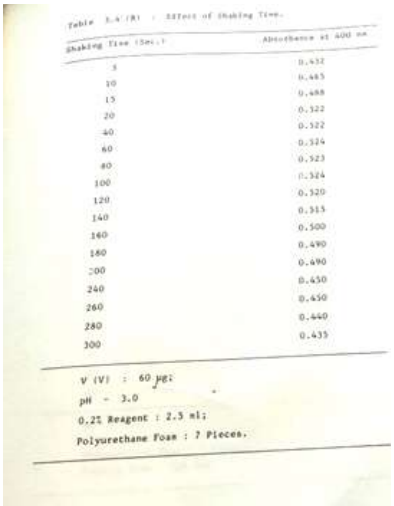

Table 3.4 (B) : Effect of Shaking Time.

Shaking Time (Sec.)	Absorbance at 400 nm
5	0.432
10	0.465
15	0.488
20	0.522
40	0.522
60	0.524
80	0.523
100	0.524
120	0.520
140	0.515
160	0.500
180	0.490
200	0.490
240	0.450
260	0.450
280	0.440
300	0.435

V (V) : 60 µg;
pH - 3.0
0.2% Reagent : 2.5 ml;
Polyurethane Foam : 7 Pieces.

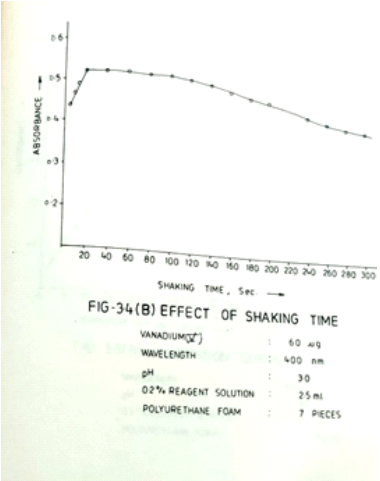

Calibration Curve for Vandium (V)

Under the optimum conditions as specified in the recommended procedure the calibration curve was obtained. The results are shown in table. Beer's law was obeyed in therange 5-90microg. The molar absorptivity was found to be $2.310*10^{4}$ $lmol^{-1}$ cm^{-1} at 400nm and sensitivity being $1.58 * 10^{-2}$ of vanadium (V) for the absorbance of 0.001
Results are shown in following table and figures

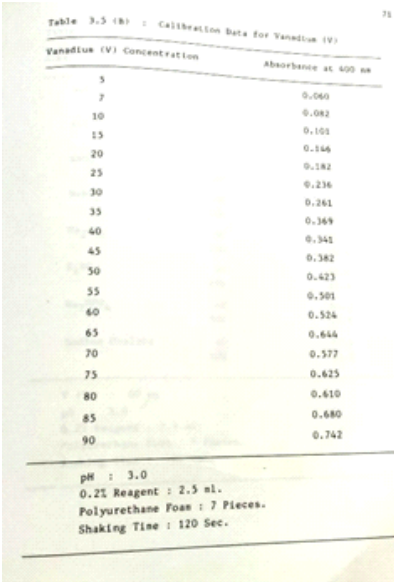

Table 3.5 (B) : Calibration Data for Vanadium (V)

Vanadium (V) Concentration	Absorbance at 400 nm
5	
7	0.060
10	0.082
15	0.101
20	0.146
25	0.182
30	0.236
35	0.261
40	0.369
45	0.341
50	0.382
55	0.423
60	0.501
65	0.524
70	0.644
75	0.577
80	0.625
85	0.610
90	0.680
	0.742

pH : 3.0
0.2% Reagent : 2.5 ml.
Polyurethane Foam : 7 Pieces.
Shaking Time : 120 Sec.

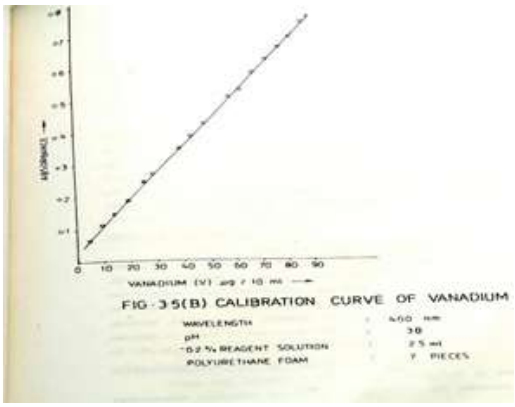

Precision

Ten samples of the solution containing 60microg of vanadium (V) were prepared by diluting the stock solution and the complex formed with the reagent was obtained. The absorbance was measured at 400nm. Mean absorbance of 0.524 with a standard deviation of 0.28% was obtained.

References:

1. A.V. peterburgskii , V.S. Kudryashov, E. E. Tormasava: Chem. Abstr. 84,29718k (1976)
2. Siegel helmut, : Metal Ions in Biological Systems" 6, Marcel Dekker, New York (1976)

3. Horvath, " Trace elements and health in trace substances and health" ed. Newberne, P. M Marcel Dekker, Part 1,319 (1976)
4. Hopkins Cannon, Alfred , Rose, Geoghem, Environ, 2, i93 (1977): CHem. 87, 109, 146496 (1977)
5. N. A. Telvitie : Anal Chem. 325, 604 (1953)
6. F.H. Hulcher; Anal. Chem.32,1183 (1960)
7. U. Priyadarshini, S..G. Tandon; Anat. Chem.33,435 (1961)
8. F.Feige; "Spot tests in inorganic Analysis", %th Ed., Elsevier, New York,123 (1970)
9. D.P.S Rathore and P.K. tarafder; J. Ind. Chem.Sic. 68,179 (1991)
10. R.K .Chug, Manjeet Kumar and D.P>s Rathore; J. Ind. Chem. Soc.70, 87,Jan.(1993).
11. A.K.Rana and J.P. Shah; J.Ind.Chem.Soc.58,1100(1981)
12. A.K.Kalra, M.B.Singh and R.P singh; J. Ind. Chem. Soc. 60,226 (1983)
13. S.P. mathur, M.R. Bhandari; Proc.Ind.Sci.congree,64,(1973)
14. H. sankegowda and G. rekha;J.Ind.Chem.Soc.10.623 (1987)
15. M.Satake and Y.Takagi;Bunseki Kagaku,26,386 (1977)